

**Space-time Finite Element Methods for
Parabolic Initial-Boundary Problems
with Variable Coefficients**

Andreas Schafelner

DK-Report No. 2017-07

09 2017

A-4040 LINZ, ALTENBERGERSTRASSE 69, AUSTRIA

Supported by

Austrian Science Fund (FWF)



FWF

Der Wissenschaftsfonds.

Upper Austria



Editorial Board: Bruno Buchberger
Bert Jüttler
Ulrich Langer
Manuel Kauers
Esther Klann
Peter Paule
Clemens Pechstein
Veronika Pillwein
Silviu Radu
Ronny Ramlau
Josef Schicho
Wolfgang Schreiner
Franz Winkler
Walter Zulehner

Managing Editor: Silviu Radu

Communicated by: Ulrich Langer
Bert Jüttler

DK sponsors:

- **Johannes Kepler University Linz (JKU)**
- **Austrian Science Fund (FWF)**
- **Upper Austria**

Space-time Finite Element Methods for Parabolic Initial-Boundary Problems with Variable Coefficients

Andreas Schafelner
Institute for Computational Mathematics, Linz

September 22, 2017

Abstract

We introduce a conforming space-time finite element method for the numerical solution of parabolic initial-boundary value problems with variable, possibly discontinuous diffusion coefficients. Discontinuous diffusion coefficients allow the treatment of moving interfaces. We show stability of the method and an a priori error estimates, including the case of local stabilizations which are important for adaptivity. The performed numerical tests validate the theoretical results.

1 Introduction

When we deal with physical problems, for instance, diffusion problems, heat-conduction problems, or simulations of electrical machines, the governing partial differential equations (PDEs) are often of parabolic type. Thus, the development of numerical schemes to solve parabolic equations is of great importance. The standard approach for solving parabolic PDEs is usually some kind of time-stepping method, with semi-discretization in the spatial variables. Another approach would be to first discretize with respect to time and then perform a discretization in the spatial variables. This approach is called Rothe's method. A more recent and alternative approach consists in a full space-time discretization at once by treating time just as another space variable, i.e., we solve a problem with one dimension more. The basic steps for these methods can be summarized in the following way:

1. Line Variational Formulation and Vertical Method of Lines:

- multiply the PDE by an appropriate test-function $v(x)$,
 - integrate over the spatial computational domain Ω ,
 - use integration by parts on the highest order spatial derivative,
 - discretize first in space by some spatial discretization like finite element method (FEM), and then solve the resulting first-order system of ordinary differential equations in time with an appropriate time-stepping method, e.g., a Runge-Kutta method.
2. Line Variational Formulation and Horizontal Method of Lines (Rothe's method):
- multiply by the PDE an appropriate test-function $v(x)$,
 - integrate over the spatial computational domain Ω ,
 - use integration by parts on the highest order spatial derivative,
 - discretize first in time by some time-stepping method like the implicit Euler scheme, and then discretize the resulting sequence of elliptic problems by means of an appropriate discretization method like the FEM.
3. Space-time Variational Formulation:
- multiply the PDE by an appropriate test-function $v(x, t)$,
 - integrate over the space-time domain (cylinder) $\mathcal{Q} = \Omega \times (0, T)$,
 - use integration by parts, e.g. on the highest order spatial derivative and/or the temporal derivative,
 - discretize in space and time simultaneously, e.g., by space-time FEM or Isogeometric Analysis (IgA), and solve the resulting linear system by an efficient solver.

In this paper, we will focus on the latter approach. The motivation behind this is that, for elliptic problems, there exist plenty of efficient and, most important, parallel solving methods. If we would be able to derive a stable discrete bilinear form, for which we can prove coercivity (ellipticity) in some mesh-dependent norm in the space-time FE-space, then we can solve the space-time problem fully in parallel. Another reason for the space-time approach is that we are not restricted to a special structure of the mesh. This means that we can apply adaptive mesh refinement both in space and time simultaneously. Last but not least, we can easily deal with moving interfaces and domains, where the coefficients of the PDE and/or the spatial domain

Ω_t depend on the time as well. Under certain assumptions imposed on the movement, we can transform the time dependent spatial domain to a fixed spatial domain via a change of variables (see [12, Chapter III, §1]).

The standard discretization techniques, namely the vertical method of lines and Rothe's method, and their properties are well investigated, see [25] and [13], respectively. However, their sequential structure complicates the parallel solution of the resulting discretized problem, the development of efficient space-time adaptive methods, as well as the treatment of moving interfaces and spatial domains. The application of a space-time finite element scheme has already a long history, see e.g. [6, 9]. However, the analysis of the equivalent operator equations was done more recently, see, e.g. [21, 27, 15]. Another popular approach are time-parallel multigrid methods [7]. Most of the more recent space-time finite element methods use discontinuous Galerkin methods, at least in time, see, e.g., [16, 17, 18, 24], and the references given therein. But also conforming space-time methods have been developed, e.g., Steinbach introduced a stable Petrov-Galerkin method [22], and Touloupoulos uses bubble functions to stabilise a Galerkin method [26]. In the context of using Isogeometric Analysis as space-time discretization method, Langer, Moore and Neumüller [14] proposed a space-time method for parabolic evolution equations.

The main aim of this paper is to generalize the results for a space-time scheme proposed by Langer, Moore and Neumüller in [14], where the authors use IgA for the discretization, to the case of moving interfaces, i.e., t -dependent, discontinuous diffusion coefficients and the possibility to chose local (element-wise) stabilisations of the form $v_h + \theta_E h_E \partial_t v_h$ depending on the mesh-size h_E of an element E from the finite element mesh. Instead of IgA, we will use a conforming finite element method (FEM) to discretize the parabolic initial-boundary value problem, which we specify in the following. Let $\mathcal{Q} = \mathcal{Q}_T := \Omega \times (0, T)$ be the space-time cylinder, with $\Omega \subset \mathbb{R}^d$, $d \in \{1, 2, 3\}$, being a sufficiently smooth and bounded spatial domain, and $T > 0$ being the final time. Furthermore, let $\Sigma := \partial\Omega \times (0, T)$, $\overline{\Sigma}_0 := \overline{\Omega} \times \{0\}$ and $\overline{\Sigma}_T := \overline{\Omega} \times \{T\}$ such that $\partial\mathcal{Q} = \Sigma \cup \overline{\Sigma}_0 \cup \overline{\Sigma}_T$. Then we consider the following model problem that can formally be written as follows: Given f , g , ν and u_0 , find u such that (s.t.)

$$\frac{\partial u}{\partial t}(x, t) - \operatorname{div}_x(\nu(x, t)\nabla_x u(x, t)) = f(x, t), \quad (x, t) \in \mathcal{Q}, \quad (1.1)$$

$$u(x, t) = g(x, t) = 0, \quad (x, t) \in \Sigma, \quad (1.2)$$

$$u(x, 0) = u_0(x) = 0, \quad x \in \overline{\Omega}, \quad (1.3)$$

where the diffusion coefficient (reluctivity in electromagnetics) ν is a given uniformly positive and bounded coefficient. The dependence of ν not only

on space but also on time enables us to model moving interfaces. Note that we do not require ν to be smooth. In fact, we will admit discontinuities for ν . For simplicity, we assume homogeneous Dirichlet boundary and initial conditions.

The paper is structured in the following way: In Section 2, we will consider the existence and uniqueness of a weak solution to the parabolic initial boundary value problem (1.1)-(1.3). In Section 3, we will derive a stable discrete variational formulation and the space-time finite element scheme. Moreover, we will derive an a priori error estimate. In Section 4, we present the test cases for which we have performed the numerical studies, whereas, in Section 5, we discuss the numerical results. Section 6 contains conclusions and outlook on the future work.

2 The Space-time variational formulation

Before we proceed in deriving a stable finite-element scheme to solve the parabolic initial-boundary value problem (1.1)-(1.3), we have to ensure the existence and uniqueness of a solution, and, moreover, to which class the solution belongs. For this, we use the theory presented by Ladyžhenskaya in [12, p.116ff], restricted to our model problem. But first let us define the proper spaces.

Definition 1. Let $L_2(\mathcal{Q}_T)$ be space of square integrable functions in the space-time domain \mathcal{Q}_T . Then we define the following Sobolev (Hilbert) spaces

$$\begin{aligned} H_0^1(\mathcal{Q}_T) &= W_{2,0}^1(\mathcal{Q}_T) := \{u \in L_2(\mathcal{Q}_T) : \nabla u \in L_2(\mathcal{Q}_T) \wedge u|_{\Sigma} = 0\}, \\ H^{1,0}(\mathcal{Q}_T) &= W_2^{1,0}(\mathcal{Q}_T) := \{u \in L_2(\mathcal{Q}_T) : \nabla_x u \in L_2(\mathcal{Q}_T)\}, \\ \mathring{H}^{1,0}(\mathcal{Q}_T) &= \mathring{W}_2^{1,0}(\mathcal{Q}_T) := \{u \in H^{1,0}(\mathcal{Q}_T) : u|_{\Sigma} = 0\}, \end{aligned}$$

equipped with the usual scalar products and norms, as well as the Banach space

$$V_2(\mathcal{Q}_T) := \{u \in H^{1,0}(\mathcal{Q}_T) : |u|_{\mathcal{Q}_T} < \infty\},$$

with subspaces

$$\begin{aligned} \mathring{V}_2(\mathcal{Q}_T) &:= \{u \in \mathring{H}^{1,0}(\mathcal{Q}_T) : |u|_{\mathcal{Q}_T} < \infty\}, \\ V_2^{1,0}(\mathcal{Q}_T) &:= \{u \in V_2(\mathcal{Q}_T) : \lim_{\Delta t \rightarrow 0} \|u(\cdot, t + \Delta t) - u(\cdot, t)\|_{L_2(\Omega)} = 0, \text{ uniformly on } [0, T]\}, \\ \mathring{V}_2^{1,0}(\mathcal{Q}_T) &:= V_2^{1,0}(\mathcal{Q}_T) \cap \mathring{H}^{1,0}(\mathcal{Q}_T), \end{aligned}$$

where the norm $|\cdot|_{\mathcal{Q}_T}$ is defined by

$$|u|_{\mathcal{Q}_t} := \max_{0 \leq \tau \leq t} \|u(\cdot, \tau)\|_{L_2(\Omega)} + \|\nabla_x u\|_{\mathcal{Q}_t}. \quad (2.1)$$

Here, the appearing differential operators are defined as follows:

$$\nabla = (\nabla_x, \nabla_t)^T, \quad \nabla_x = (\partial_{x_1}, \dots, \partial_{x_d})^T \quad \text{and} \quad \nabla_t = (\partial_t).$$

Now let us consider the model problem: Find u s.t.

$$\mathcal{M}u \equiv \partial_t u - \operatorname{div}(\nu \nabla_x u) = f \text{ in } \mathcal{Q}_T, \quad (2.2)$$

$$u = 0 \text{ on } \Sigma, \quad u = \varphi \text{ on } \Sigma_0, \quad (2.3)$$

with given data

$$\varphi \in L_2(\Omega) \quad \text{and} \quad f \in L_{2,1}(\mathcal{Q}_T) := \{v : \int_0^T \|v(\cdot, t)\|_{L_2(\Omega)} dt < \infty\}, \quad (2.4)$$

and a uniformly bounded coefficient

$$0 < \underline{\nu} \leq \nu(x, t) \leq \bar{\nu}, \quad \text{for almost all } (x, t) \in \mathcal{Q}_T, \quad (2.5)$$

where $\underline{\nu}$ and $\bar{\nu} = \text{const.} > 0$. To show now the existence of a weak solution in an appropriate function space, we use Galerkin's method. We formally start with multiplying the PDE by the solution u and integrate over the truncated space-time domain $\mathcal{Q}_t = \Omega \times (0, t)$, $t \in (0, T)$, i.e.,

$$\int_{\mathcal{Q}_t} \mathcal{M}u \cdot u \, dxdt = \int_{\mathcal{Q}_t} f u \, dxdt. \quad (2.6)$$

Using integration by parts, the homogeneous boundary condition on the lateral boundary Σ and $\vec{n}_x = 0$ on $\Sigma_0 \cup \Sigma_t$, where $\Sigma_t := \Omega \times \{t\}$, we obtain

$$\begin{aligned} \int_{\mathcal{Q}_t} \mathcal{M}u \cdot u \, dxdt &= \int_{\mathcal{Q}_t} \partial_t u u - \operatorname{div}_x(\nu(x, t) \nabla_x u) \, dxdt = \\ &= \int_{\mathcal{Q}_t} \frac{1}{2} \partial_t (u^2) \, dxdt + \int_{\mathcal{Q}_t} \nu(x, t) |\nabla_x u|^2 \, dxdt, \end{aligned}$$

for the left hand side of (2.6). Now we use Gauss' theorem and the fact that $n_t \equiv 0$ on Σ to get rid of the time derivative and we obtain the following identity

$$\frac{1}{2} \|u(\cdot, t)\|_{L_2(\Omega)}^2 + \int_{\mathcal{Q}_t} \nu(x, t) |\nabla_x u|^2 \, dxdt = \frac{1}{2} \|u(\cdot, 0)\|_{L_2(\Omega)}^2 + \int_{\mathcal{Q}_t} f u \, dxdt. \quad (2.7)$$

We call (2.7) *energy balance equation*. From this equation, we will derive a bound for u in some specific norm $|\cdot|_{\mathcal{Q}_t}$. First, we estimate the left hand side (lhs) of (2.7) from below by

$$\frac{1}{2}\|u(\cdot, t)\|_{L_2(\Omega)}^2 + \int_{\mathcal{Q}_t} \nu(x, t) |\nabla_x u|^2 \, dx dt \geq \frac{1}{2}\|u(\cdot, t)\|_{L_2(\Omega)}^2 + \underline{\nu} \int_{\mathcal{Q}_t} |\nabla_x u|^2 \, dx dt,$$

and the right hand side (rhs) of (2.7) from above by

$$\begin{aligned} \frac{1}{2}\|u(\cdot, 0)\|_{L_2(\Omega)}^2 + \int_{\mathcal{Q}_t} f u \, dx dt &= \frac{1}{2}\|u(\cdot, 0)\|_{L_2(\Omega)}^2 + \int_0^t \int_{\Omega} f(x, \tau) u(x, \tau) \, dx \, d\tau \\ &\leq \frac{1}{2}\|u(\cdot, 0)\|_{L_2(\Omega)}^2 + \int_0^t \|f(\cdot, \tau)\|_{L_2(\Omega)} \|u(\cdot, \tau)\|_{L_2(\Omega)} \, d\tau \\ &\leq \frac{1}{2}\|u(\cdot, 0)\|_{L_2(\Omega)}^2 + \int_0^t \|f(\cdot, \tau)\|_{L_2(\Omega)} \max_{\sigma \in [0, t]} \|u(\cdot, \sigma)\|_{L_2(\Omega)} \, d\tau \\ &\leq \frac{1}{2}\|u(\cdot, 0)\|_{L_2(\Omega)}^2 + \|f\|_{2,1,\mathcal{Q}_t} \max_{\tau \in [0, t]} \|u(\cdot, \tau)\|_{L_2(\Omega)}. \end{aligned}$$

Combining these two estimates gives us

$$\frac{1}{2}\|u(\cdot, t)\|_{L_2(\Omega)}^2 + \underline{\nu} \|\nabla_x u\|_{\mathcal{Q}_t}^2 \leq \|u(\cdot, 0)\|_{L_2(\Omega)}^2 + \max_{0 \leq \tau \leq t} \|u(\cdot, \tau)\|_{L_2(\Omega)} \|f\|_{2,1,\mathcal{Q}_t}. \quad (2.8)$$

Denoting $\max_{0 \leq \tau \leq t} \|u(\cdot, \tau)\|_{L_2(\Omega)}$ by $y(t)$ and multiplying (2.8) by 2, we obtain

$$\|u(\cdot, t)\|_{L_2(\Omega)}^2 + 2\underline{\nu} \|\nabla_x u\|_{\mathcal{Q}_t}^2 \leq y(t) \|u(\cdot, 0)\|_{L_2(\Omega)} + 2y(t) \|f\|_{2,1,\mathcal{Q}_t} = j(t),$$

where we used the estimate $\|u(\cdot, 0)\|_{L_2(\Omega)}^2 \leq \max_{0 \leq \tau \leq t} \|u(\cdot, \tau)\|_{L_2(\Omega)} \|u(\cdot, 0)\|_{L_2(\Omega)}$. From this, we deduce two inequalities, i.e.,

$$y(t)^2 \leq j(t) \quad \text{and} \quad \|\nabla_x u\|_{\mathcal{Q}_t}^2 \leq (2\underline{\nu})^{-1} j(t). \quad (2.9)$$

The second estimate can easily be verified, whereas the first one is obtained by estimating the lhs from below by $\|u(\cdot, t)\|_{L_2(\Omega)}^2$. This expression holds for any $\tau \in [0, t]$, hence it holds also for the maximum. However, the only terms in $j(t)$ depending on t are $y(t)$, where we already take a maximum over $[0, t]$. Thus, the first expression of (2.9) follows. We now take the square-root of both expressions in (2.9) and add them up to obtain

$$|u|_{\mathcal{Q}_t} := y(t) + \|\nabla_x u\|_{\mathcal{Q}_t} \leq \left(1 + \frac{1}{2\underline{\nu}}\right)^{1/2} |u|_{\mathcal{Q}_t}^{1/2} (\|u(\cdot, 0)\|_{L_2(\Omega)} + 2\|f\|_{2,1,\mathcal{Q}_t})^{1/2}. \quad (2.10)$$

We bring similar terms on the same side and take the square on each side of the inequality. Thus we have obtained an upper bound for $|u|_{\mathcal{Q}_t}$ in the form

$$|u|_{\mathcal{Q}_t} \leq \left(1 + \frac{1}{2\nu}\right)^{-1} (\|u(\cdot, 0)\|_{L_2(\Omega)} + 2\|f\|_{2,1,\mathcal{Q}_t}) =: c\mathcal{F}(t), \quad (2.11)$$

which holds for any $t \in [0, T]$. However, this bound requires a solution where point evaluation with respect to (wrt) time is well defined. Before we proof that our problem (2.2) has such a weak solution, we have to introduce a suitable definition of the weak solution.

Definition 2. A function $u \in \mathring{H}^{1,0}(\mathcal{Q}_T)$ is called a generalized (weak) solution in $H^{1,0}(\mathcal{Q}_T)$ of the parabolic initial-boundary value problem (2.2) - (2.3) if it satisfies the identity

$$\begin{aligned} \mathcal{M}(u, v) &\equiv \int_{\mathcal{Q}_T} -u\partial_t v + \nu(x, t)\nabla_x u \nabla_x v \, dx dt \\ &= \int_{\Omega} \varphi v(\cdot, 0) \, dx + \int_{\mathcal{Q}_T} f v \, dx dt, \end{aligned} \quad (2.12)$$

for all $v \in \hat{H}_0^1(\mathcal{Q}_T) := \{v \in H_0^1(\mathcal{Q}_T) : v = 0 \text{ on } \Sigma_T\}$.

To proof solvability of (2.2) in this class, i.e. solvability of (2.12), we will use Galerkin's method. Let $\{\varphi_j\}$ be a L_2 -orthonormal fundamental system in $\mathring{W}_2^1(\Omega)$. In (2.2), we substitute u with an appropriate test function u^N , multiply the obtained equation by each φ_j for $j = 1, \dots, N$ and integrate wrt x over Ω . We use integration by parts in the principle term, and obtain a system of N equations

$$(\partial_t u^N, \varphi_j) + (\nu(\cdot, t)\nabla_x u, \nabla_x \varphi_j) = (f, \varphi_j), \quad (2.13)$$

where $(\cdot, \cdot) = (\cdot, \cdot)_{L_2(\Omega)}$ is the standard $L_2(\Omega)$ scalar product. In (2.13), we express u^N with the fundamental system $\{\varphi_j\}$, i.e., $u^N(x, t) := \sum_{j=1}^N c_j^N(t)\varphi_j(x)$. We can rewrite (2.13) wrt the coefficient functions $c_i(t) = c_i^N(t)$,

$$\sum_{j=1}^N \frac{d}{dt} c_j(t) \underbrace{(\varphi_j, \varphi_i)}_{\delta_j^i} + \sum_{j=1}^N c_j(t) (\nu(\cdot, t)\nabla_x \varphi_j, \nabla_x \varphi_i) = (f(\cdot, t), \varphi_i), \text{ for } i = 1, \dots, N, \quad (2.14)$$

with the initial condition

$$\sum_{j=1}^N c_j(0) (\varphi_j, \varphi_i) = (\varphi, \varphi_i), \quad (2.15)$$

that is nothing but the L_2 -projection to $\text{span}\{\varphi_1, \dots, \varphi_N\}$. This system is a system of N linear ordinary differential equations with principal terms $\frac{d}{dt}c_i(t)$ and bounded coefficient functions in front of the zero-order terms $c_i(t)$. This system has a unique solution of absolutely continuous functions $c_1^N(t), \dots, c_N^N(t)$ (see [8, IX, 60.2]), which uniquely define the approximate solution u^N . Now, we want to derive a bound for the series u^N . To do so, we first multiply each equation in (2.13) with the corresponding solution coefficient $c_l^N(t)$, $l = 1, \dots, N$ and sum these equations up from 1 to N . We proceed by integrating this sum over $(0, t)$ and obtain an equation of the form (2.7) for u^N , i.e.,

$$\frac{1}{2}\|u^N(\cdot, t)\|_{L_2(\Omega)}^2 + \int_{\mathcal{Q}_t} \nu(x, t)|\nabla_x u^N| \, dx dt = \frac{1}{2}\|u^N(\cdot, 0)\|_{L_2(\Omega)}^2 + \int_{\mathcal{Q}_t} f u^N \, dx dt. \quad (2.16)$$

We can derive a bound for $|u^N|_{\mathcal{Q}_T}$ from (2.16) in the same manner as we did for $|u|_{\mathcal{Q}_T}$ from (2.7), i.e.,

$$|u^N|_{\mathcal{Q}_t} \leq c(\|u^N(\cdot, 0)\|_{L_2(\Omega)} + 2\|f\|_{2,1,\mathcal{Q}_t}).$$

Furthermore, we know the upper bound $\|u^N(\cdot, 0)\|_{L_2(\Omega)} \leq \|\varphi\|_{L_2(\Omega)}$. Therefore, we obtain the bound

$$|u^N|_{\mathcal{Q}_T} \leq \tilde{c}, \quad (2.17)$$

where \tilde{c} is a constant independent of N . Hence the sequence $\{u^N\}$ is a bounded sequence in the Hilbert space $L_2(\mathcal{Q}_T)$. This can easily be deduced from (2.17) and Definition 1. Hilbert spaces are reflexive spaces. Thus, $\{u^N\}$ has a weakly convergent subsequence $\{u^{N_k}\}$. The same holds true for its derivatives $\{\nabla_x u^N\}$ with $\{\nabla_x u^{N_k}\}$. Therefore, $\{u^{N_k}\}$ and $\{\nabla_x u^{N_k}\}$ converge weakly to some unique element $u \in \hat{H}^{1,0}(\mathcal{Q}_T)$. Is this u the desired generalized (weak) solution of our model problem (2.2) - (2.3)? Let us again multiply (2.13) by some arbitrary absolutely continuous functions $d_l(t)$ with $\frac{d}{dt}d_l \in L_2(0, T)$, with $d_l(T) = 0$. We sum the obtained equations up from 1 to N , integrate over the interval $(0, T)$ and perform integration by parts with respect to time. The resulting equation is

$$\int_{\mathcal{Q}_T} -u^N \partial_t \Phi + \nu(x, t) \nabla_x u^N \nabla_x \Phi \, dx dt = \int_{\Omega} u^N \Phi|_{t=0} \, dx + \int_{\mathcal{Q}_T} f \Phi \, dx dt, \quad (2.18)$$

for $\Phi(x, t) = \sum_{k=1}^N d_k(t) \varphi_k(x)$. The set of all such functions Φ with the desired properties of d_l is denoted by \mathfrak{M}_N . The superset $\bigcup_{p=1}^{\infty} \mathfrak{M}_p$ is dense in $\hat{H}_0^1(\mathcal{Q}_T)$ (see [12]). We fix a $\Phi \in \mathfrak{M}_p$ and take the limit of (2.18) for $N_k \geq p$,

i.e.,

$$\int_{\mathcal{Q}_T} \underbrace{-u^{N_k} \partial_t \Phi}_{\rightarrow u \partial_t \Phi} + \nu(x, t) \underbrace{\nabla_x u^N \nabla_x \Phi}_{\rightarrow \nabla_x u \nabla_x \Phi} \, dx dt = \int_{\Omega} \underbrace{u^N \Phi|_{t=0}}_{\rightarrow \varphi \Phi|_{t=0}} \, dx + \int_{\mathcal{Q}_T} f \Phi \, dx dt. \quad (2.19)$$

We obtain exactly the definition of a generalized (weak) solution (2.12), with $v = \Phi \in \mathfrak{M}$. As these union of all such spaces is dense in $\hat{H}_0^1(\mathcal{Q}_T)$, the equation (2.19) holds for any $v \in \hat{H}_0^1(\mathcal{Q}_T)$. Thus u is indeed a generalized solution of our model problem (2.2) - (2.3). We gather these results in the following theorem.

Theorem 3 ([12, Chapter III, Thm. 3.1]). *Under the conditions (2.4) and (2.5), the problem (2.2)-(2.3) has at least one generalized (weak) solution in $\hat{H}^{1,0}(\mathcal{Q}_T)$, as defined in Definition 2.*

Proof. Follows from the derivation above. \square

We know now that at least one solution u exists, but is this solution unique? To prove this, we will make again use of the results presented by Ladyžhenskaya in [12, Chapter III, §2]. First, we consider our generalized solution u as a generalized solution in $L_2(\mathcal{Q}_T)$ of the problem

$$\partial_t u - \Delta u = \tilde{f} + \operatorname{div}_x(\mathbf{F}) \quad \text{in } \mathcal{Q}_T, \quad (2.20)$$

$$u|_{t=0} = \phi(x) \text{ for } x \in \Omega, \quad u|_{\Sigma} = 0, \quad (2.21)$$

with $\tilde{f} \equiv f$ and $\mathbf{F}_i = \nu(x, t) \nabla_x u - \nabla_x u$. Hence, by [12, Chapter III, Thm. 2.2 & Thm. 2.3], it follows that $u(x, t)$ is a generalized solution of (2.20) - (2.21) in $\mathring{V}_2^{1,0}(\mathcal{Q}_T)$. By this, we can define a new class of generalised solutions.

Definition 4 ([12, Chapter III]). A generalised solution $u \in \hat{H}^{1,0}$ of (2.2) - (2.3) is called a generalized solution of (2.2) - (2.3) in $\mathring{V}_2^{1,0}(\mathcal{Q}_T)$, if $u \in \mathring{V}_2^{1,0}(\mathcal{Q}_T)$ and it fulfils the energy-balance equation (2.7) and the identity

$$\begin{aligned} \int_{\Omega} u(x, t) v(x, t) \, dx - \int_{\Omega} \varphi v(x, 0) \, dx \\ + \int_{\mathcal{Q}_t} -u \partial_t v + \nu \nabla_x u \nabla_x v \, dx dt = \int_{\mathcal{Q}_t} f v \, dx dt, \end{aligned} \quad (2.22)$$

for all $v \in H_0^1(\mathcal{Q}_T)$ and any $t \in (0, T)$.

We will show uniqueness of the problem (2.2) - (2.3) in $H^{1,0}(\mathcal{Q}_T)$ as usual by contradiction. Let $u_1 \neq u_2 \in \mathring{H}^{1,0}(\mathcal{Q}_T)$ be two generalised solutions of (2.2) - (2.3), then the difference $u := u_1 - u_2$ is also a generalised solution of (2.2) - (2.3), but with homogeneous initial data and zero right hand side. Moreover, by what we have shown above, it is also a generalised solution in $\mathring{V}_2^{1,0}(\mathcal{Q}_T)$, so it satisfies (2.7) with zero right hand side. If it satisfies (2.7), we have shown that its norm $|u|_{\mathcal{Q}_T}$ is subject to the bound (2.11), but also with zero right hand side. We obtain $u = u_1 - u_2 \equiv 0$, which is a contradiction to our assumption $u_1 \neq u_2$. Moreover, the operator B , which assigns each tuple (f, φ) its generalised solution in $\mathring{V}_2^{1,0}(\mathcal{Q}_T)$ is linear and the energy balance equation (2.7) can be obtained from the identity (2.22) (see [12]). We can summarise the results in the following theorem.

Theorem 5 ([12, Chapter III, Thm. 3.2]). *If the assumptions (2.4) and (2.5) are fulfilled, then any generalised solution of (2.2)-(2.3) in $\mathring{H}^{1,0}(\mathcal{Q}_T)$ is the generalised solution in $\mathring{V}_2^{1,0}(\mathcal{Q}_T)$ and it is unique in $\mathring{H}^{1,0}(\mathcal{Q}_T)$.*

Corollary 6. *If the assumptions (2.4) and (2.5) hold, then there exists a unique generalized solution $u \in \mathring{H}^{1,0}(\mathcal{Q}_T) \cap \mathring{V}_2^{1,0}(\mathcal{Q}_T)$ to the problem (2.2) - (2.3).*

3 The Space-time finite element scheme

From the previous section, we know that there exists a unique generalized solution of the initial-boundary value problem (1.1) in $\mathring{H}^{1,0}(\mathcal{Q}) \cap \mathring{V}_2^{1,0}(\mathcal{Q})$. The goal of this section is to derive a stable space-time finite element scheme with a coercive (elliptic) discrete bilinear form, and, therefore, to ensure existence and uniqueness of a finite element solution. Similar to Langer, Moore and Neumüller in [14], we use special time-upwind test functions that are locally scaled in our case. First, we need a regular triangulation \mathcal{T}_h of our space-time domain \mathcal{Q} (for details, see e.g. [1, 3]). We formally define this triangulation as

$$\mathcal{T}_h := \{E : E \subset \mathcal{Q}, E \text{ open}\} \quad (3.1)$$

with the properties

$$\overline{\mathcal{Q}} = \bigcup_{E \in \mathcal{T}_h} \overline{E} \quad \text{and} \quad E \cap E' = \emptyset \text{ for } E \neq E' \in \mathcal{T}_h. \quad (3.2)$$

On each of these elements E , we define individual *time upwind test functions*

$$v_{h,t}(x, t) := v_h(x, t) + \theta_E h_E \partial_t v_h(x, t), \text{ for all } (x, t) \in E, \quad (3.3)$$

where θ_E is a positive parameter that will be defined later, and $h_E := \text{diam}(E)$. Here, v_h is some test function from a standard conforming finite element space V_{0h} , e.g., $V_{0h} = \{v \in C(\overline{\mathcal{Q}}) : v|_E \in \mathbb{P}_p \subset \mathbb{Q}_p\}$ that is considered in this paper. From now on, unless specified otherwise, all functions depend on both space and time variables. So, we can omit the arguments. In this section we will make use of the following spaces:

$$V_0 = H_{0,\underline{0}}^{1,1}(\mathcal{Q}) := \{u \in L_2(\mathcal{Q}) : \nabla_x u \in L_2(\mathcal{Q}), \partial_t u \in L_2(\mathcal{Q}) \text{ and } u|_{\Sigma \cup \Sigma_0} = 0\}, \quad (3.4)$$

$$H_{0,\underline{0}}^{2,1}(\mathcal{T}_h) := \{v \in H_{0,\underline{0}}^{1,1}(\mathcal{Q}) : v|_E \in H^{2,1}(E), \forall E \in \mathcal{T}_h\}, \quad (3.5)$$

$$W_\infty^1(\mathcal{T}_h) := \{v \in L_\infty(\mathcal{Q}) : v|_E \in W_\infty^1(E), \forall E \in \mathcal{T}_h\}. \quad (3.6)$$

We assume that $\nu \in W_\infty^1(\mathcal{T}_h)$ and that the PDE has a sufficiently smooth solution u , e.g., $u \in H_{0,\underline{0}}^{2,1}(\mathcal{T}_h)$. Then we proceed in the usual manner, i.e., we first multiply the PDE (1.1) by our space-time test function $v_{h,t}$, and then integrate over a single element E , obtaining

$$\int_E (\partial_t u - \text{div}_x(\nu \nabla_x u)) v_{h,t} \, d(x, t) = \int_E f v_{h,t} \, d(x, t).$$

Summing up over all elements and applying integration by parts on the principle term, we obtain

$$\begin{aligned} & \sum_{E \in \mathcal{T}_h} \int_E \partial_t u v_{h,t} + \nu \nabla_x u \nabla_x v_{h,t} \, d(x, t) - \int_{\partial E} \nu \nabla_x u \cdot \vec{n}_x v_{h,t} \, ds_{(x,t)} = \\ & \sum_{E \in \mathcal{T}_h} \int_E \partial_t u v_h + \theta_E h_E \partial_t u \partial_t v_h + \nu \nabla_x u \nabla_x v_h + \theta_E h_E \nu \nabla_x u \nabla_x (\partial_t v_h) \, d(x, t) \\ & \quad - \int_{\partial E} \nu \nabla_x u \cdot \vec{n}_x v_h + \theta_E h_E \nu \nabla_x u \cdot \vec{n}_x \partial_t v_h \, ds_{(x,t)}, \end{aligned}$$

for the left hand side, while the right hand side remains unchanged. For the exact solution u of (1.1), we know that the fluxes have to be continuous, i.e., let E and E' be two adjacent elements, then

$$(\nu \nabla_x u \cdot \vec{n}_x)|_E = (\nu \nabla_x u \cdot \vec{n}_x)|_{E'}. \quad (3.7)$$

From this, we know that one part of the boundary terms vanishes from all inner edges, i.e. we obtain

$$\sum_{E \in \mathcal{T}_h} \int_E \partial_t u v_h + \theta_E h_E \partial_t u \partial_t v_h + \nu \nabla_x u \nabla_x v_h + \theta_E h_E \nu \nabla_x u \nabla_x (\partial_t v_h) \, d(x, t)$$

$$\begin{aligned}
& - \sum_{\substack{E \in \mathcal{T}_h \\ \partial E \cap \partial \mathcal{Q} \neq \emptyset}} \int_{\partial E} \nu \nabla_x u \cdot \vec{n}_x v_h \, ds_{(x,t)} - \sum_{E \in \mathcal{T}_h} \int_{\partial E} \nu \theta_E h_E \nabla_x u \cdot \vec{n}_x \partial_t v_h \, ds_{(x,t)} \\
& = \sum_{E \in \mathcal{T}_h} \int_E f(v_h + \theta_E h_E \partial_t v_h) \, d(x,t).
\end{aligned}$$

We require v_h to be zero on Σ , and know that \vec{n}_x vanishes on Σ_0 and Σ_T . Therefore, the first boundary term completely disappears from our equation, and we obtain

$$\begin{aligned}
& \sum_{E \in \mathcal{T}_h} \int_E [\partial_t u v_h + \theta_E h_E \partial_t u \partial_t v_h + \nu \nabla_x u \nabla_x v_h + \theta_E h_E \nu \nabla_x u \nabla_x (\partial_t v_h)] \, d(x,t) \\
& - \sum_{E \in \mathcal{T}_h} \int_{\partial E} \nu \theta_E h_E \nabla_x u \cdot \vec{n}_x \partial_t v_h \, ds_{(x,t)} = \sum_{E \in \mathcal{T}_h} \int_E f(v_h + \theta_E h_E \partial_t v_h) \, d(x,t).
\end{aligned}$$

We now arrived at the consistency identity for (1.1)

$$a_h(u, v_h) = l_h(v_h), \quad \forall v_h \in V_{0h}, \quad (3.8)$$

that holds for a sufficiently smooth solution u , e.g., $u \in H_{0,0}^{2,1}(\mathcal{T}_h)$, where

$$\begin{aligned}
a_h(u, v_h) & := \sum_{E \in \mathcal{T}_h} \int_E \partial_t u v_h + \theta_E h_E \partial_t u \partial_t v_h \, d(x,t) \\
& + \int_E \nu \nabla_x u \cdot \nabla_x v_h + \theta_E h_E \nu \nabla_x u \cdot \nabla_x (\partial_t v_h) \, d(x,t) \quad (3.9) \\
& - \int_{\partial E} \theta_E h_E \nu \nabla_x u \cdot \vec{n}_x \partial_t v_h \, ds_{(x,t)},
\end{aligned}$$

$$l_h(v_h) := \sum_{E \in \mathcal{T}_h} \int_E f(v_h + \theta_E h_E \partial_t v_h) \, d(x,t), \quad (3.10)$$

with given $\nu \in W_\infty^1(\mathcal{T}_h)$ and $f \in L_2(\mathcal{Q})$.

Remark 7. We can derive an equivalent scheme to (3.9). In particular, we perform the same steps as above, but instead of applying integration by parts on both principal terms, we only apply it to the first principal term and keep the second. Hence we obtain another consistency identity for (1.1)

$$\tilde{a}_h(u, v_h) = l_h(v_h), \quad \forall v_h \in V_{0h},$$

that holds for a sufficiently smooth solution u , e.g., $u \in H_{0,0}^{2,1}(\mathcal{T}_h)$, where

$$\tilde{a}_h(u, v_h) := \sum_{E \in \mathcal{T}_h} \int_E \partial_t u v_h + \theta_E h_E \partial_t u \partial_t v_h \, d(x,t)$$

$$+ \int_E \nu \nabla_x u \cdot \nabla_x v_h + \theta_E h_E \operatorname{div}_x(\nu \nabla_x u) \partial_t v_h \, d(x, t)$$

with given $\nu \in W_\infty^1(\mathcal{T}_h)$ and $f \in L_2(\mathcal{Q})$, and l_h as in (3.10).

Remark 8. *If the test functions $v_h \in V_{0h}$ are continuous and piecewise linear ($p = 1$), then the term in (3.9) containing $\nabla_x(\partial_t v_h)$ vanishes in all elements $E \in \mathcal{T}_h$, since it only contains mixed second order derivatives.*

Now we look for a Galerkin approximation $u_h \in V_{0h}$ to the generalized solution u of our initial boundary value problem (1.1)-(1.3) using the variational identity (3.8), i.e., find $u_h \in V_{0h}$ such that

$$a_h(u_h, v_h) = l_h(v_h), \quad \forall v_h \in V_{0h}, \quad (3.11)$$

with a_h and l_h as defined above by (3.9) and (3.10), respectively. In Section 2, we already showed existence and uniqueness of a weak solution to the initial-boundary value problem (1.1)-(1.3). However, our discrete variational problem (3.11) is of a different form. Thus, we have to investigate the stability of the space-time finite element scheme. More precisely, we will even show ellipticity of the bilinear form $a_h(\cdot, \cdot) : V_{0h} \times V_{0h} \rightarrow \mathbb{R}$ wrt the mesh-dependent norm

$$\|v_h\|_h^2 := \sum_{E \in \mathcal{T}_h} [\|\nu^{1/2} \nabla_x v_h\|_{L_2(E)}^2 + \theta_E h_E \|\partial_t v_h\|_{L_2(E)}^2] + \frac{1}{2} \|v_h\|_{L_2(\Sigma_T)}^2. \quad (3.12)$$

For the following derivations, we assume that our triangulation \mathcal{T}_h of \mathcal{Q} is *shape regular* such that the local approximation error estimates are available, [1, 3]. The triangulation \mathcal{T}_h of \mathcal{Q} is called quasi-uniform, if there exists a constant c_u such that

$$h_E \leq h \leq c_u h_E, \quad \text{for all } E \in \mathcal{T}_h, \quad (3.13)$$

where $h = \max_{E \in \mathcal{T}_h} h_E$. Moreover, we introduce localised bounds for our coefficient function ν , i.e.,

$$\underline{\nu}_E \leq \nu(x, t) \leq \bar{\nu}_E, \quad \text{for almost all } (x, t) \in E \text{ and for all } E \in \mathcal{T}_h, \quad (3.14)$$

where $\underline{\nu}_E$ and $\bar{\nu}_E = \text{const.} > 0$. In the following, we need some inverse inequalities for functions from finite element spaces.

Lemma 9. *There exist generic positive constants $c_{I,1}$ and $c_{I,2}$, such that*

$$\|v_h\|_{L_2(\partial E)} \leq c_{I,1} h_E^{-1/2} \|v_h\|_{L_2(E)}, \quad (3.15)$$

$$\|\nabla v_h\|_{L_2(E)} \leq c_{I,2} h_E^{-1} \|v_h\|_{L_2(E)} \quad (3.16)$$

for all $v_h \in V_{0h}$ and for all $E \in \mathcal{T}_h$.

Proof. For (3.15), see e.g. [19, 4], and for (3.16) see e.g. [1, 3, 4]. \square

From $\nabla = (\nabla_x, \partial_t)^T$ and (3.16), we can immediately deduce

$$\|\partial_t v_h\|_{L_2(E)} \leq c_{I,2} h_E^{-1} \|v_h\|_{L_2(E)}. \quad (3.17)$$

The above inequalities hold for the standard norms. However, we will also need such a result in some scaled norm.

Lemma 10. *Let $\nu \in W_\infty^1(\mathcal{T}_h)$ be a given uniformly positive function. Then*

$$\|v\|_{L_2^\nu(E)}^2 = \int_E \nu(x, t) |v(x, t)|^2 \, d(x, t)$$

is a norm and there holds the inverse estimate

$$\|\partial_t v_h\|_{L_2^\nu(E)} \leq \|\nabla v_h\|_{L_2^\nu(E)} \leq c_{I,\nu} h_E^{-1} \|v_h\|_{L_2^\nu(E)}, \quad (3.18)$$

for all $v_h \in V_{0h}$ and for all $E \in \mathcal{T}_h$.

Proof. If $\nu = \nu_E = \text{const} > 0$ on E , then (3.18) is nothing else than the classical inverse inequality (3.16). In general, we can at least assume that (3.14) holds. Using (3.14) and (3.16), we obtain

$$\begin{aligned} \|\nabla v_h\|_{L_2^\nu(E)} &\leq \sqrt{\bar{\nu}_E} \|\nabla v_h\|_{L_2(E)} \leq \sqrt{\bar{\nu}_E} c_{I,2} h_E^{-1} \|v_h\|_{L_2(E)} \\ &\leq \underbrace{\left(\frac{\bar{\nu}_E}{\underline{\nu}_E} \right)^{1/2}}_{=: c_{I,\nu}} c_{I,2} h_E^{-1} \|v_h\|_{L_2^\nu(E)} \end{aligned}$$

It is clear that in $1 \leq \bar{\nu}_E/\underline{\nu}_E$ is close to 1 in practical applications. \square

Below, we will need the estimate

$$\|\partial_t \partial_{x_i} v_h\|_{L_2^\nu(E)} \leq c_{I,\nu} h_E^{-1} \|\partial_{x_i} v_h\|_{L_2^\nu(E)}, \quad (3.19)$$

which obviously holds for all $v_h \in V_{0h}$ and for all $E \in \mathcal{T}_h$. Moreover, we need the following inverse inequality.

Lemma 11. *Let $\nu \in W_\infty^1(\mathcal{T}_h)$ be a given uniformly positive function. Let $W_h|_E := \{w_h : w_h = \nabla_x v_h, v_h \in V_{0h}|_E\}$. Then there holds the inverse estimate*

$$\|\operatorname{div}_x(\nu w_h)\|_{L_2(E)} \leq c_{I,3} h_E^{-1} \|\nu w_h\|_{L_2(E)}, \quad \forall w_h \in W_h|_E, \quad (3.20)$$

where $c_{I,3}$ is a positive constant, independent of h_E .

Proof. First, we know that $V_{0h}|_E$ is a finite space spanned by the local shape functions $\{p^{(i)}\}_{i \in \omega_E}$. Hence the space $W_h|_E$ is also finite and spanned by the generating system $\{\nabla_x p^{(i)}\}_{i \in \omega_E}$. Moreover, for a fixed ν , each product $z_h := \nu w_h$ can be represented by means of a non-necessary unique linear combination $\{\nu \nabla_x p^{(i)}\}_{i \in \omega_E}$ on E . We denote this space by $Z_h(E) := \text{span}_{i \in \omega_E} \{\nu \nabla_x p^{(i)}\}$. Using Cauchy's inequality, we obtain

$$\begin{aligned} \|\text{div}_x z_h\|_{L_2(E)}^2 &= \int_E |\text{div}_x z_h|^2 \, d(x, t) = \int_E \left| \sum_{i=1}^d \partial_{x_i} z_{h,i} \right|^2 \, d(x, t) \\ &\leq d \int_E \sum_{i=1}^d |\partial_{x_i} z_{h,i}|^2 \, d(x, t) = d \sum_{i=1}^d \|\partial_{x_i} z_{h,i}\|_{L_2(E)}^2, \end{aligned}$$

for all $z_h \in Z_h(E)$. Now, by a simple scaling argument, we can estimate each element in the sum and obtain

$$\begin{aligned} d \sum_{i=1}^d \|\partial_{x_i} z_{h,i}\|_{L_2(E)}^2 &\leq d \sum_{i=1}^d C^2 h_E^{-2} \|z_{h,i}\|_{L_2(E)}^2 \\ &= d C^2 h_E^{-2} \|z_h\|_{L_2(E)}^2. \end{aligned}$$

Indeed, transforming to the reference triangle, using the norm equivalence on finite dimensional spaces, and transforming back to E , we obtain

$$\begin{aligned} \|\partial_{x_i} z_{h,i}\|_{L_2(E)}^2 &\leq \|\nabla z_{h,i}\|_{L_2(E)}^2 = \int_E |\nabla z_{h,i}|^2 \, d(x, t) \\ &\leq c h_E^{d+1} \int_{\Delta} |\nabla \hat{z}_{h,i}|^2 \, d(\xi, \tau) \leq c h_E^{d+1} h_E^{-2} \int_{\Delta} |\hat{\nabla} \hat{z}_{h,i}|^2 \, d(\xi, \tau) \\ &\leq C h_E^{-2} \int_E |z_{h,i}|^2 \, d(x, t) = C h_E^{-2} \|z_{h,i}\|_{L_2(E)}. \end{aligned}$$

Taking the square root and setting $c_{I,3} := C\sqrt{d}$ closes the proof. \square

Lemma 11 gives information how the two norms involved scale wrt the mesh-size h_E . However, the estimate (3.20) is not sharp wrt the constant.

Lemma 12. *Let the assumptions of Lemma 11 hold. Then*

$$\|\text{div}_x(\nu w_h)\|_{L_2(E)} \leq c_{opt} \|\nu w_h\|_{L_2(E)}, \quad \forall w_h \in W_h|_E \quad (3.21)$$

with $c_{opt}^2 = \sup_{0 \neq z_h \in Z_h(E)} \frac{\|\text{div}_x(z_h)\|_{L_2(E)}^2}{\|z_h\|_{L_2(E)}^2}$.

Proof. From Lemma 11 we know that there must be a constant c such that

$$\|\operatorname{div}_x(z_h)\|_{L_2(E)} \leq c\|z_h\|_{L_2(E)} \quad \forall z_h \in Z_h(E).$$

With the assumption $z_h \neq 0$ we can rewrite the inequality above as

$$\frac{\|\operatorname{div}_x(z_h)\|_{L_2(E)}^2}{\|z_h\|_{L_2(E)}^2} \leq c^2.$$

Now we immediately see that the optimal value for c is nothing else than the supremum of the expression on left hand side, i.e.,

$$c_{opt}^2 := \sup_{0 \neq z_h \in Z_h(E)} \frac{\|\operatorname{div}_x(z_h)\|_{L_2(E)}^2}{\|z_h\|_{L_2(E)}^2}.$$

What remains is to ensure that this supremum is finite. We start by identifying the kernel of $\|\nu \nabla_x \cdot\|_{L_2(E)}$. Using the notation of the proof of Lemma 11, we know

$$\begin{aligned} 0 &= \|z_h\|_{L_2(E)} = \left\| \sum_{i \in \omega_E} z_i q^{(i)} \right\|_{L_2(E)} \\ &= \left\| \sum_{i \in \omega_E} z_i \nu \nabla_x p^{(i)} \right\|_{L_2(E)} = \|\nu \nabla_x \underbrace{\sum_{i \in \omega_E} z_i p^{(i)}}_{=\varphi}\|_{L_2(E)}. \end{aligned}$$

This identity holds if and only if $\nabla_x \varphi \equiv 0$, i.e., if $\varphi = \varphi(t)$. Now let $\varphi \in \ker \|\nu \nabla_x \cdot\|_{L_2(E)}$. Then we immediately deduce that

$$\|\operatorname{div}_x(z_h)\|_{L_2(E)} = \|\operatorname{div}_x(\nu \nabla_x \sum_{i \in \omega_E} z_i p^{(i)})\|_{L_2(E)} = \|\operatorname{div}_x(\underbrace{\nu \nabla_x \varphi}_{=0})\|_{L_2(E)} = 0,$$

i.e., $\ker \|\nu \nabla_x \cdot\|_{L_2(E)} \subset \ker \|\operatorname{div}_x(\nu \nabla_x \cdot)\|_{L_2(E)}$. \square

Remark 13. Note that the constant c_{opt} in Lemma 12 is not only optimal but also computable. Let $z_h \in Z_h(E)$, then by definition we have

$$z_h(x, t) = \sum_{j \in \tilde{\omega}_E} \tilde{z}_j \tilde{q}^{(j)}.$$

Here we assume that the $\{\tilde{q}^{(j)}\}_{j \in \tilde{\omega}_E}$ form a basis of $Z_h(E)$. Moreover, we know

$$\|z_h\|_{L_2(E)}^2 = (z_h, z_h)_{L_2(E)} \quad \text{and} \quad \|\operatorname{div}_x z_h\|_{L_2(E)}^2 = \underbrace{(\operatorname{div}_x z_h, \operatorname{div}_x z_h)_{L_2(E)}}_{=: b(z_h, z_h)}.$$

As our space $Z_h(E)$ is finite, we can further rewrite these scalar products. Let $y_h, z_h \in Z_h(E)$, then

$$(y_h, z_h)_{L_2(E)} = \sum_{i \in \tilde{\omega}_E} (y_h, \tilde{q}^{(i)})_{L_2(E)} \tilde{z}_i = \sum_{i, j \in \tilde{\omega}_E} \tilde{y}_j (\tilde{q}^{(j)}, \tilde{q}^{(i)})_{L_2(E)} \tilde{z}_i.$$

This can be interpreted as

$$(y_h, z_h)_{L_2(E)} = (M_h \underline{y}, \underline{z})_{\ell_2}, \quad \text{with} \quad (M_h)_{ij} = (\tilde{q}^{(j)}, \tilde{q}^{(i)})_{L_2(E)},$$

where \underline{y} and \underline{z} are the vector of coefficients wrt the basis. By the same argument we obtain

$$b(y_h, z_h) = (B_h \underline{y}, \underline{z})_{\ell_2}, \quad \text{with} \quad (B_h)_{ij} = b(\tilde{q}^{(j)}, \tilde{q}^{(i)})_{L_2(E)}.$$

Combining the above identities, we get with $N_E = |\omega_E|$

$$c_{opt}^2 = \sup_{0 \neq z_h \in Z_h(E)} \frac{\|\operatorname{div}_x(z_h)\|_{L_2(E)}^2}{\|z_h\|_{L_2(Q_T)(E)}^2} = \sup_{\underline{z} \in \mathbb{R}^{N_E}} \frac{(B_h \underline{z}, \underline{z})_{\ell_2}}{(M_h \underline{z}, \underline{z})_{\ell_2}}. \quad (3.22)$$

Hence, c_{opt}^2 is the largest eigenvalue of the generalised eigenvalue problem

$$B_h \underline{z} = \lambda M_h \underline{z}.$$

Now, we are able to proof the following lemma.

Lemma 14. *There exists a constant μ_a such that*

$$a_h(v_h, v_h) \geq \mu_a \|v_h\|_h^2, \quad \forall v_h \in V_{0h}, \quad (3.23)$$

with $\mu_a = \min_{E \in \mathcal{T}_h} \{1 - c_{I,3} \sqrt{\frac{\bar{\nu}_E \theta_E}{4h_E}}\} \geq \frac{1}{2}$ for $\theta_E \leq \frac{h_E}{c_{I,3}^2 \bar{\nu}_E}$, i.e., $\mu_a = \frac{1}{2}$ for $\theta_E = \frac{h_E}{c_{I,3}^2 \bar{\nu}_E}$.

Proof. We first do integration by parts at the last term, obtaining

$$\begin{aligned} a_h(v_h, v_h) &= \sum_{E \in \mathcal{T}_h} \int_E \frac{1}{2} \partial_t(v_h^2) + \theta_E h_E (\partial_t v_h)^2 + \nu |\nabla_x v_h|^2 \, d(x, t) \\ &\quad + \int_E \theta_E h_E \nu \nabla_x v_h \nabla_x \partial_t v_h \, d(x, t) - \int_{\partial E} \theta_E h_E \nu \nabla_x v_h \vec{n}_x \partial_t v_h \, ds_{(x,t)} \\ &= \sum_{E \in \mathcal{T}_h} \int_E \frac{1}{2} \partial_t(v_h^2) \, d(x, t) + \theta_E h_E \|\partial_t v_h\|_{L_2(E)}^2 + \int_E \nu |\nabla_x v_h|^2 \, d(x, t) \\ &\quad - \int_E \theta_E h_E \operatorname{div}_x(\nu \nabla_x v_h) \partial_t v_h \, d(x, t) \end{aligned}$$

Now using Gauss' theorem and the facts that v_h is continuous across the element boundary and that $n_t = 0$ on Σ , we obtain

$$\begin{aligned}
a_h(v_h, v_h) &= \sum_{E \in \mathcal{T}_h} \int_{\partial E} \frac{1}{2} v_h^2 n_t \, ds_{(x,t)} + \theta_E h_E \|\partial_t v_h\|_{L_2(E)}^2 \\
&\quad + \int_E \nu |\nabla_x v_h|^2 - \theta_E h_E \operatorname{div}_x(\nu \nabla_x v_h) \partial_t v_h \, d(x,t) \\
&= \frac{1}{2} (\|v_h\|_{L_2(\Sigma_T)}^2 - \|v_h\|_{L_2(\Sigma_0)}^2) + \sum_{E \in \mathcal{T}_h} \theta_E h_E \|\partial_t v_h\|_{L_2(E)}^2 \\
&\quad + \int_E \nu |\nabla_x v_h|^2 - \theta_E h_E \operatorname{div}_x(\nu \nabla_x v_h) \partial_t v_h \, d(x,t)
\end{aligned}$$

The first, second and third term already appear in the definition of our mesh-dependent norm (3.12). What remains is to estimate the last term. Using the Cauchy-Schwarz inequality, Lemma 11 and a scaled Young's inequality, we arrive at the estimates

$$\begin{aligned}
|\theta_E h_E \int_E \operatorname{div}_x(\nu \nabla_x v_h) \partial_t v_h \, d(x,t)| &\leq \theta_E h_E \|\operatorname{div}_x(\nu \nabla_x v_h)\|_{L_2(E)} \|\partial_t v_h\|_{L_2(E)} \\
&\leq \theta_E h_E c_{I,3} h_E^{-1} \|\nu \nabla_x v_h\|_{L_2(E)} h_E^{-1/2} h_E^{1/2} \|\partial_t v_h\|_{L_2(E)} \\
&\leq c_{I,3} \left(\frac{\varepsilon \bar{\nu}_E \theta_E}{2h_E} \|\nabla_x v_h\|_{L_2^{\nu}(E)}^2 + \frac{1}{2\varepsilon} \theta_E h_E \|\partial_t v_h\|_{L_2(E)}^2 \right).
\end{aligned}$$

Using this estimate in the equality above and the fact that $v_h = 0$ on Σ_0 , we get

$$\begin{aligned}
a_h(v_h, v_h) &\geq \frac{1}{2} \|v_h\|_{L_2(\Sigma_T)}^2 + \sum_{E \in \mathcal{T}_h} \left[\left(1 - \frac{c_{I,3}}{2\varepsilon}\right) \theta_E h_E \|\partial_t v_h\|_{L_2(E)}^2 \right. \\
&\quad \left. + \left(1 - \varepsilon \frac{c_{I,3} \bar{\nu}_E \theta_E}{2h_E}\right) \|\nabla_x v_h\|_{L_2^{\nu}(E)}^2 \right].
\end{aligned}$$

Now we choose $\varepsilon = \sqrt{h_E / (\theta_E \bar{\nu}_E)}$ and obtain

$$\begin{aligned}
a_h(v_h, v_h) &\geq \min_{E \in \mathcal{T}_h} \left(1 - c_{I,3} \sqrt{\frac{\theta_E \bar{\nu}_E}{4h_E}}\right) \\
&\quad \times \left(\sum_{E \in \mathcal{T}_h} \left[\|\nabla_x v_h\|_{L_2^{\nu}(E)}^2 + \theta_E h_E \|\partial_t v_h\|_{L_2(E)}^2 \right] + \frac{1}{2} \|v_h\|_{L_2(\Sigma_T)}^2 \right) \\
&\geq \mu_a \|v_h\|_h^2,
\end{aligned}$$

which concludes the first part of the proof. The second assertion can be shown by a simple calculation, i.e.,

$$1 - c_{I,3} \sqrt{\frac{\theta_E \bar{\nu}_E}{4h_E}} \geq \frac{1}{2} \Leftrightarrow c_{I,3} \sqrt{\frac{\theta_E \bar{\nu}_E}{4h_E}} \leq \frac{1}{2}$$

$$\begin{aligned} &\Leftrightarrow c_{I,3}^2 \frac{\theta_E \bar{\nu}_E}{h_E} \leq 1 \\ &\Leftrightarrow \theta_E \leq \frac{h_E}{\bar{\nu}_E c_{I,3}^2}. \end{aligned}$$

□

Remark 15. *The above proof does hold for any polynomial degree $p \geq 1$ of v_h and any fixed, uniformly positive $\nu \in L_\infty(\mathcal{Q})$. However, for the special case $p = 1$ and $\nu|_E = \text{const}$, the above proof is trivial, since*

$$\partial_t(\nabla_x v_h) \equiv 0 \quad \text{and} \quad \nu|_E \Delta_x v_h \equiv 0.$$

Hence, there holds the identity

$$\begin{aligned} a_h(v_h, v_h) &= \sum_{E \in \mathcal{T}_h} \int_E \partial_t v_h v_h + \theta_E h_E (\partial_t v_h)^2 + \nu |\nabla_x v_h|^2 \, d(x, t) \\ &= \sum_{E \in \mathcal{T}_h} \frac{1}{2} \int_{\partial E} v_h^2 n_t \, ds_{(x,t)} + \theta_E h_E \|\partial_t v_h\|_{L_2(E)}^2 \|\nabla_x v_h\|_{L_2^2(E)}^2 \\ &= \|v_h\|_h^2, \end{aligned}$$

i.e., $\mu_a = 1$. Moreover, we immediately deduce that for this special case, the choice of θ_E has no influence on the ellipticity of the space-time finite element method.

Remark 16. *An alternative approach to the proof of Lemma 14 consists of not applying integration by parts on the last two terms of (3.9), but instead estimate*

$$\theta_E h_E \int_E \nu \nabla_x v_h \nabla_x (\partial_t v_h) \, d(x, t) \quad \text{and} \quad \theta_E h_E \int_{\partial E} \nu \nabla_x v_h \vec{n}_x \partial_t v_h \, ds_{(x,t)}$$

separately.

Lemma 14 already ensures uniqueness of the finite element solution $u_h \in V_{0h}$. Furthermore, since we use the same trial- and test-space V_{0h} , and this space is finite dimensional, uniqueness implies existence of finite element solution $u_h \in V_{0h}$ of (3.8).

For the special case of uniform meshes and uniform θ , i.e., $h_E = h$ and $\theta_E = \theta$ for all $E \in \mathcal{T}_h$, and $\nu \equiv 1$, a proof for ellipticity with a *mesh-independent* constant was done by Langer et.al.[14]. For a second special case, where θ_E vanishes, i.e., $\theta_E = \theta = 0$ for all $E \in \mathcal{T}_h$, Steinbach in [22] has shown existence and uniqueness of both the continuous and discrete version

of (3.8). In addition, both papers include also a priori error estimates, where Steinbach's estimate is based on a discrete inf-sup condition.

To show an a priori error estimate wrt the mesh dependent norm (3.12), we need to show that our bilinear form $a_h(\cdot, \cdot)$ is uniformly bounded on $V_{0h,*} \times V_{0h}$, where $V_{0h,*} = H_0^{1,0}(\mathcal{Q}) \cap H^2(\mathcal{T}_h) + V_{0h}$ with the norm

$$\begin{aligned} \|v\|_{h,*}^2 &= \|v\|_h^2 + \sum_{E \in \mathcal{T}_h} [(\theta_E h_E)^{-1} \|v\|_{L_2(E)}^2 + \theta_E h_E |v|_{H^2(E)}^2] \\ &= \frac{1}{2} \|v\|_{L_2(\Sigma_T)}^2 + \sum_{E \in \mathcal{T}_h} [\theta_E h_E \|\partial_t v\|_{L_2(E)}^2 + \|\nabla_x v\|_{L_2'(E)}^2] \\ &\quad + (\theta_E h_E)^{-1} \|v\|_{L_2(E)}^2 + \theta_E h_E |v|_{H^2(E)}^2 \end{aligned} \quad (3.24)$$

Moreover, we will make use of the following scaled trace inequality.

Lemma 17. *There exists a positive constants $c_{Tr} > 0$ such that*

$$\|v\|_{L_2(\partial E)}^2 \leq 2c_{Tr}^2 h_E^{-1} (\|v\|_{L_2(E)}^2 + h_E^2 \|\nabla v\|_{L_2(E)}^2) \quad (3.25)$$

for all $v \in H^1(E), \forall E \in \mathcal{T}_h$.

Proof. See e.g. [19]. □

Lemma 18. *The discrete bilinear form $a_h(\cdot, \cdot)$ is uniformly bounded on $V_{0h,*} \times V_{0h}$, i.e.,*

$$|a_h(u, v_h)| \leq \mu_b \|u\|_{h,*} \|v_h\|_h, \quad (3.26)$$

where $\mu_b = \max_{E \in \mathcal{T}_h} \{2(1 + \theta_E h_E^{-1} c_{Tr}^2 \frac{\bar{v}_E^2}{\underline{v}_E^2}), 2c_{Tr}^2 \bar{v}_E^2, 2 + c_{I,1}^2, 1 + (c_{I,\nu} \theta_E)^2\}^{1/2}$ that is bounded provided that $\theta_E = \mathcal{O}(h_E)$.

Proof. We will estimate the bilinear form (3.9) term by term. For the first term, since $V_{0h} \subset H_{0,\bar{0}}^{1,1}(\mathcal{Q})$, we can apply integration by parts and the Cauchy-Schwarz inequality, and obtain

$$\begin{aligned} \sum_{E \in \mathcal{T}_h} \int_E \partial_t u v_h \, d(x, t) &= \sum_{E \in \mathcal{T}_h} \left[- \int_E u \partial_t v_h \, d(x, t) + \int_{\partial E} u n_t v_h \, ds_{(x,t)} \right] \\ &\leq \sum_{E \in \mathcal{T}_h} \left[((\theta_E h_E)^{-1} \|u\|_{L_2(E)}^2)^{1/2} ((\theta_E h_E \|\partial_t v_h\|_{L_2(E)}^2)^{1/2}] \right. \\ &\quad \left. + (\|u\|_{L_2(\Sigma_T)}^2)^{1/2} (\|v_h\|_{L_2(\Sigma_T)}^2)^{1/2} \right]. \end{aligned}$$

For the second and third term, applying the Cauchy-Schwarz inequality for each term of the sum yields

$$\theta_E h_E \int_E \partial_t u \partial_t v_h \, d(x, t) \leq (\theta_E h_E \|\partial_t u\|_{L_2(E)}^2)^{1/2} (\theta_E h_E \|\partial_t v_h\|_{L_2(E)}^2)^{1/2},$$

$$\int_E \nu \nabla_x u \nabla_x v_h \, d(x, t) \leq (\|\nabla_x u\|_{L^2_\nu(E)})^{1/2} (\|\nabla_x v_h\|_{L^2_\nu(E)})^{1/2},$$

respectively. For the fourth term, we use again Cauchy-Schwarz' inequality, the inverse estimate (3.19), and obtain

$$\begin{aligned} \theta_E h_E \int_E \nu \nabla_x u \nabla_x (\partial_t v_h) \, d(x, t) &\leq (\|\nabla_x u\|_{L^2_\nu(E)})^{1/2} ((\theta_E h_E)^2 \|\partial_t \nabla_x v_h\|_{L^2_\nu(E)})^{1/2} \\ &= (\|\nabla_x u\|_{L^2_\nu(E)})^{1/2} ((\theta_E h_E)^2 \sum_{i=1}^d \|\partial_t (\partial_{x_i} v_h)\|_{L^2_\nu(E)})^{1/2} \\ &\leq (\|\nabla_x u\|_{L^2_\nu(E)})^{1/2} ((\theta_E h_E)^2 \sum_{i=1}^d c_{I,\nu}^2 h_E^{-2} \|\partial_{x_i} v_h\|_{L^2_\nu(E)})^{1/2} \\ &= (\|\nabla_x u\|_{L^2_\nu(E)})^{1/2} ((c_{I,\nu} \theta_E)^2 \|\nabla_x v_h\|_{L^2_\nu(E)})^{1/2}. \end{aligned}$$

For the last term, we apply Cauchy-Schwarz and the trace inequalities (3.17) and (3.25), and get

$$\begin{aligned} \theta_E h_E \int_{\partial E} \nu \nabla_x u \vec{n}_x \partial_t v_h \, ds_{(x,t)} &\leq (\theta_E \bar{\nu}_E^2 \|\nabla_x u\|_{L_2(\partial E)})^{1/2} (\theta_E h_E^2 \|\partial_t v_h\|_{L_2(\partial E)})^{1/2} \\ &\leq (2\theta_E \bar{\nu}_E^2 c_{Tr}^2 h_E^{-1} [\|\nabla_x u\|_{L_2(E)}^2 + h_E^2 \sum_{i=1}^d \|\nabla \partial_{x_i} u\|_{L_2(E)}^2])^{1/2} \\ &\quad \times (\theta_E h_E c_{I,1}^2 \|\partial_t v_h\|_{L_2(E)})^{1/2} \\ &\leq \left(2\theta_E c_{Tr}^2 \frac{\bar{\nu}_E^2}{\underline{\nu}_E} h_E^{-1} \|\nabla_x u\|_{L^2_\nu(E)}^2 + 2c_{Tr}^2 \bar{\nu}_E^2 \theta_E h_E |u|_{H^2(E)}^2 \right)^{1/2} \\ &\quad \times \left(c_{I,1}^2 \theta_E h_E \|\partial_t v_h\|_{L_2(E)}^2 \right)^{1/2}. \end{aligned}$$

Now we combine the above terms, apply Cauchy's inequality and gather all similar items, i.e.,

$$\begin{aligned} |a_h(u, v_h)| &\leq (\|u\|_{L_2(\Sigma_T)})^{1/2} (\|v_h\|_{L_2(\Sigma_T)})^{1/2} \\ &\quad + \sum_{E \in \mathcal{T}_h} \left[((\theta_E h_E)^{-1} \|u\|_{L_2(E)}^2)^{1/2} (\theta_E h_E \|\partial_t v_h\|_{L_2(E)})^{1/2} \right. \\ &\quad + (\theta_E h_E \|\partial_t u\|_{L_2(E)})^{1/2} (\theta_E h_E \|\partial_t v_h\|_{L_2(E)})^{1/2} \\ &\quad + (\|\nabla_x u\|_{L^2_\nu(E)})^{1/2} (\|\nabla_x v_h\|_{L^2_\nu(E)})^{1/2} \\ &\quad \left. + (\|\nabla_x u\|_{L^2_\nu(E)})^{1/2} ((c_{I,\nu} \theta_E)^2 \|\nabla_x v_h\|_{L^2_\nu(E)})^{1/2} \right] \end{aligned}$$

$$\begin{aligned}
& + \left(2\theta_E c_{Tr}^2 \frac{\bar{\nu}_E}{\underline{\nu}_E} h_E^{-1} \|\nabla_x u\|_{L^2_\nu(E)}^2 + 2c_{Tr}^2 \theta_E \bar{\nu}_E h_E |u|_{H^2(E)}^2 \right)^{1/2} \\
& \quad \times \left(c_{I,1}^2 \theta_E h_E \|\partial_t v_h\|_{L_2(E)}^2 \right)^{1/2} \\
& \leq \left(\|u\|_{L_2(\Sigma_T)}^2 + \sum_{E \in \mathcal{T}_h} \left[\theta_E h_E \|\partial_t u\|_{L_2(E)}^2 + 2(1 + \theta_E c_{Tr}^2 \frac{\bar{\nu}_E}{\underline{\nu}_E} h_E^{-1}) \|\nabla_x u\|_{L^2_\nu(E)}^2 \right. \right. \\
& \quad \left. \left. + (\theta_E h_E)^{-1} \|u\|_{L_2(E)}^2 + 2c_{Tr}^2 \bar{\nu}_E^2 \theta_E h_E |u|_{H^2(E)}^2 \right] \right)^{1/2} \\
& \quad \times \left(\|v_h\|_{L_2(\Sigma_T)}^2 + \sum_{E \in \mathcal{T}_h} \left[(2 + c_{I,1}^2) \theta_E h_E \|\partial_t v_h\|_{L_2(E)}^2 \right. \right. \\
& \quad \left. \left. + (1 + (c_{I,1} \theta_E)^2) \|\nabla_x v_h\|_{L^2_\nu(E)}^2 \right] \right)^{1/2} \\
& \leq \underbrace{\max_{E \in \mathcal{T}_h} \left\{ 2(1 + \theta_E h_E^{-1} c_{Tr}^2 \frac{\bar{\nu}_E}{\underline{\nu}_E}), 2c_{Tr}^2 \bar{\nu}_E^2, 2 + c_{I,1}^2, 1 + (c_{I,\nu} \theta_E)^2 \right\}}_{=: \mu_b}^{1/2} \|u\|_{h,*} \|v_h\|_h.
\end{aligned}$$

Choosing now $\theta_E = \mathcal{O}(h_E)$ ensures the boundedness of the constant μ_b . \square

Remark 19. Choosing θ_E as in Lemma 14, i.e., $\theta_E = h_E / (c_{I,3}^2 \bar{\nu}_E)$, we obtain $\mu_a = 1/2$ and $\mu_b = \max_{E \in \mathcal{T}_h} \left\{ 2(1 + \frac{\bar{\nu}_E c_{Tr}^2}{\underline{\nu}_E c_{I,3}^2}), 2c_{Tr}^2 \bar{\nu}_E^2, 2 + c_{I,1}^2, 1 + (\frac{c_{I,\nu} h_E}{c_{I,3}^2 \bar{\nu}_E})^2 \right\}^{1/2}$.

Remark 20. As in Remark 15, we can provide a simplified estimate for the special case $p = 1$ and $\nu|_E = \nu_E = \text{const}$. The first three terms can be estimated as in the above proof. The fourth term completely vanishes, since $\nabla_x(\partial_t v_h) = 0$. For the fifth term, we use the fact that $\partial_t v_h = \text{const}$, Gauss' theorem and the Cauchy-Schwarz inequality, obtaining

$$\begin{aligned}
\theta_E h_E \int_{\partial E} \nu_E \nabla_x u \cdot \vec{n}_x \partial_t v_h \, ds_{(x,t)} &= \theta_E h_E \nu_E \partial_t v_h \int_{\partial E} \nabla_x u \cdot \vec{n}_x \, ds_{(x,t)} \\
&= \theta_E h_E \nu_E \partial_t v_h \int_E \text{div}_x(\nabla_x u) \, d(x,t) \\
&= \theta_E h_E \nu_E \int_E \Delta_x u \partial_t v_h \, d(x,t) \\
&\leq (\theta_E h_E \nu_E^2 \|\Delta_x u\|_{L_2(E)}^2)^{1/2} (\theta_E h_E \|\partial_t v_h\|_{L_2(E)}^2)^{1/2}.
\end{aligned}$$

Gathering the terms from the proof and the above estimate, we obtain

$$|a_h(u, v_h)| \leq (\|u\|_{L_2(\Sigma_T)}^2)^{1/2} (\|v_h\|_{L_2(\Sigma_T)}^2)^{1/2}$$

$$\begin{aligned}
& + \sum_{E \in \mathcal{T}_h} \left[((\theta_E h_E)^{-1} \|u\|_{L_2(E)}^2)^{1/2} (\theta_E h_E \|\partial_t v_h\|_{L_2(E)}^2)^{1/2} \right. \\
& \quad + (\theta_E h_E \|\partial_t u\|_{L_2(E)}^2)^{1/2} (\theta_E h_E \|\partial_t v_h\|_{L_2(E)}^2)^{1/2} \\
& \quad + (\|\nabla_x u\|_{L_2^\nu(E)}^2)^{1/2} (\|\nabla_x v_h\|_{L_2^\nu(E)}^2)^{1/2} \\
& \quad \left. + (\theta_E \nu_E^2 \|\Delta_x u\|_{L_2(E)}^2)^{1/2} (\theta_E h_E \|\partial_t v_h\|_{L_2(E)}^2)^{1/2} \right] \\
& \leq \left(\|u\|_{L_2(\Sigma_T)}^2 + \sum_{E \in \mathcal{T}_h} [\theta_E h_E \|\partial_t u\|_{L_2(E)}^2 + \|\nabla_x u\|_{L_2^\nu(E)}^2] \right. \\
& \quad \left. + (\theta_E h_E)^{-1} \|u\|_{L_2(E)}^2 + \nu_E^2 \theta_E h_E \|\Delta_x u\|_{L_2(E)}^2 \right)^{1/2} \\
& \quad \times \left(\|v_h\|_{L_2(\Sigma_T)}^2 \right. \\
& \quad \left. + \sum_{E \in \mathcal{T}_h} [3\theta_E h_E \|\partial_t v_h\|_{L_2(E)}^2 + \|\nabla_x v_h\|_{L_2^\nu(E)}^2] \right)^{1/2} \\
& \leq \max_{E \in \mathcal{T}_h} \{3, \nu_E^2\}^{1/2} \|u\|_{h, **} \|v_h\|_h.
\end{aligned}$$

We immediately deduce that this new constant $\tilde{\mu}_b = \max_{E \in \mathcal{T}_h} \{3, \nu_E^2\}^{1/2}$ is also independent of h_E .

To obtain a priori error estimates wrt to the mesh dependent norm (3.12), we need interpolation error estimates for finite elements wrt (3.24), which we summarise in the next Lemmata. Moreover, we need the *broken Sobolev space*

$$H^s(\mathcal{T}_h) := \{v \in L_2(\mathcal{Q}) : v|_E \in H^s(E)\}, \quad (3.27)$$

equipped with the *broken Sobolev (semi-)norm*

$$|v|_{H^s(\mathcal{T}_h)}^2 := \sum_{E \in \mathcal{T}_h} |v|_{H^s(E)}^2 \quad \text{and} \quad \|v\|_{H^s(\mathcal{T}_h)}^2 := \sum_{E \in \mathcal{T}_h} \|v\|_{H^s(E)}^2, \quad (3.28)$$

where s is some positive integer. For further details on such spaces, we refer to [4, 19].

Lemma 21. *Let s and k be positive integers with $s \in [2, p+1]$ and $k > (d+1)/2$, respectively. Let $v \in V_0 \cap H^k(\mathcal{Q}) \cap H^s(\mathcal{T}_h)$. Then there exists an interpolation operator Π_h , mapping from $V_0 \cap H^k(\mathcal{Q})$ to V_{0h} , such that*

$$\|v - \Pi_h v\|_{L_2(E)} \leq C h_E^{s+1} |v|_{H^s(E)}, \quad (3.29)$$

$$\|\nabla(v - \Pi_h v)\|_{L_2(E)} \leq Ch_E^s |v|_{H^s(E)}, \quad (3.30)$$

$$|v - \Pi_h v|_{H^2(E)} \leq Ch_E^{s-1} |v|_{H^s(E)}, \quad (3.31)$$

where C is some generic constant independent of v . Here, p denotes the polynomial degree of the finite element basis functions.

Proof. See e.g. [2, Theorem 4.4.4] or [3, Theorem 3.1.6]. \square

Lemma 22. *Let the assumptions of Lemma 21 hold. Then the following interpolation error estimates hold:*

$$\|v - \Pi_h v\|_{L_2(\Sigma_T)} \leq c_1 \left(\sum_{\substack{E \in \mathcal{T}_h \\ \partial E \cap \Sigma_T \neq \emptyset}} h_E^{2s-1} |v|_{H^s(E)}^2 \right)^{1/2}, \quad (3.32)$$

$$\|v - \Pi_h v\|_h \leq c_2 \left(\sum_{E \in \mathcal{T}_h} h_E^{2(s-1)} |v|_{H^s(E)} \right)^{1/2}, \quad (3.33)$$

$$\|v - \Pi_h v\|_{h,*} \leq c_3 \left(\sum_{E \in \mathcal{T}_h} h_E^{2(s-1)} |v|_{H^s(E)} \right)^{1/2}. \quad (3.34)$$

The constants c_1, c_2, c_3 do not depend on h_E or v , provided that $\theta_E = \mathcal{O}(h_E)$.

Proof. We start with the first estimate (3.32). We use the scaled trace inequality (3.25), and the interpolation error estimates (3.29) and (3.30), obtaining

$$\begin{aligned} \|v - \Pi_h v\|_{L_2(\Sigma_T)}^2 &= \sum_{\substack{E \in \mathcal{T}_h \\ \partial E \cap \Sigma_T \neq \emptyset}} \|v - \Pi_h v\|_{L_2(\partial E \cap \Sigma_T)}^2 \leq \sum_{\substack{E \in \mathcal{T}_h \\ \partial E \cap \Sigma_T \neq \emptyset}} \|v - \Pi_h v\|_{L_2(\partial E)}^2 \\ &\leq \sum_{\substack{E \in \mathcal{T}_h \\ \partial E \cap \Sigma_T \neq \emptyset}} [2c_{Tr}^2 h_E^{-1} (\|v - \Pi_h v\|_{L_2(E)}^2 + h_E^2 \|\nabla(v - \Pi_h v)\|_{L_2(E)}^2)] \\ &\leq c_{Tr}^2 \sum_{\substack{E \in \mathcal{T}_h \\ \partial E \cap \Sigma_T \neq \emptyset}} [C^2 h_E^{2s-1} |v|_{H^s(E)}^2 + C^2 h_E^{2s-1} |v|_{H^s(E)}^2] \\ &\leq c_{Tr}^2 C^2 \sum_{\substack{E \in \mathcal{T}_h \\ \partial E \cap \Sigma_T \neq \emptyset}} [h_E^{2s-1} |v|_{H^s(E)}]. \end{aligned}$$

For (3.33), we use definition (3.12), assumption (3.14), the interpolation error estimate (3.30), and the above estimate (3.32), and obtain

$$\|v - \Pi_h v\|_h^2 = \sum_{E \in \mathcal{T}_h} [\theta_E h_E \|\partial_t(v - \Pi_h v)\|_{L_2(E)}^2 + \|\nabla_x(v - \Pi_h v)\|_{L_2^y(E)}^2]$$

$$\begin{aligned}
& + \frac{1}{2} \|v - \Pi_h v\|_{L_2(\Sigma_T)}^2 \\
& \leq \sum_{E \in \mathcal{T}_h} \left[\theta_E C^2 h_E^{2(s-1)} |v|_{H^s(E)}^2 + \bar{\nu}_E C^2 h_E^{2(s-1)} |v|_{H^s(E)}^2 \right] \\
& \quad + \frac{1}{2} c_1^2 \sum_{E \in \mathcal{T}_h} h_E^{2s-1} |v|_{H^s(E)}^2 \\
& \leq \sum_{E \in \mathcal{T}_h} \left[(C^2 \theta_E h_E + \bar{\nu}_E C^2 + c_1^2 h_E) h_E^{2(s-1)} |v|_{H^s(E)}^2 \right].
\end{aligned}$$

For the last estimate (3.34), we use definition (3.24), the above estimate (3.33), and the interpolation error estimate (3.31), obtaining

$$\begin{aligned}
\|v - \Pi_h v\|_{h,*}^2 & = \|v - \Pi_h v\|_h^2 + \sum_{E \in \mathcal{T}_h} \left[(\theta_E h_E)^{-1} \|v - \Pi_h v\|_{L_2(E)}^2 + \theta_E h_E |v - \Pi_h v|_{H^2(E)}^2 \right] \\
& \leq \sum_{E \in \mathcal{T}_h} \left[c_2^2 h_E^{2(s-1)} |v|_{H^s(E)}^2 + C^2 \theta_E^{-1} h_E^{2s-1} |v|_{H^s(E)}^2 + C^2 \theta_E h_E h_E^{2(s-2)} |v|_{H^s(E)}^2 \right] \\
& \leq \sum_{E \in \mathcal{T}_h} (c_2^2 + h_E \theta_E^{-1} C^2 + \theta_E h_E^{-1} C^2) h_E^{2(s-1)} |v|_{H^s(E)}^2.
\end{aligned}$$

The special choice $\theta_E = \mathcal{O}(h_E)$ ensures that the constant c_3 is independent of h_E . \square

Remark 23. *The strong assumption $v \in H^k(\mathcal{Q})$ with $k > (d+1)/2$ is needed for the interpolation error estimates for the Lagrange interpolation operator. However, in practical application this requirement is too restrictive. However, in such a practical application, the space-time cylinder $\bar{\mathcal{Q}} = \bigcup_{i=1}^M \bar{\mathcal{Q}}_i$ can be split into subdomains \mathcal{Q}_i , which correspond e.g. to different materials. On each such subdomain \mathcal{Q}_i , we can assume some regularity for $v \in H^s(\mathcal{T}(\mathcal{Q})) := \{v \in L_2(\mathcal{Q}) : v|_{\mathcal{Q}_i} \in H^s(\mathcal{Q}_i), \text{ for all } i = 1, \dots, M\}$ with some $s > 1$. For a similar case, Duan et.al. [5] have shown an interpolation error estimate of the form*

$$\|\nabla(v - I_h v)\|_{L_2(\mathcal{Q})} \leq C h^{s-1} \sum_{i=1}^M \|v\|_{H^s(\mathcal{Q}_i)},$$

where I_h is a special quasi-interpolation operator.

Now we can formulate the following a priori estimate for the error.

Theorem 24. *Let s and k be positive integers with $s \in [2, p+1]$ and $k > (d+1)/2$. Furthermore, let $u \in V_0 \cap H^k(\mathcal{Q}) \cap H^s(\mathcal{T}_h)$ be the exact solution,*

and $u_h \in V_{0h}$ the solution of the finite element scheme (3.11). Then there holds the a priori error estimate

$$\|u - u_h\|_h \leq c \left(\sum_{E \in \mathcal{T}_h} h_E^{2(s-1)} |u|_{H^s(E)}^2 \right)^{1/2}. \quad (3.35)$$

Proof. First, we know from the consistency identity (3.8) that $a_h(u, v_h) = l_h(v_h)$, and, since u_h is the approximate solution of (3.11), that $a_h(u_h, v_h) = l_h(v_h)$. Hence we have Galerkin orthogonality for our bilinear form $a_h(\cdot, \cdot)$, i.e.

$$a_h(u - u_h, v_h) = 0, \quad \forall v_h \in V_{0h}. \quad (3.36)$$

We start with the triangle inequality for the discretization error, i.e.,

$$\|u - u_h\|_h \leq \|u - \Pi_h u\|_h + \|\Pi_h u - u_h\|_h.$$

We continue by estimating the second term. Using the ellipticity proved in Lemma 14, the Galerkin orthogonality and the generalised boundedness from Lemma 18, we obtain

$$\begin{aligned} \mu_a \|\Pi_h u - u_h\|_h^2 &\leq a_h(\Pi_h u - u_h, \Pi_h u - u_h) = a_h(\Pi_h u - u, \Pi_h u - u_h) \\ &\leq \mu_b \|\Pi_h u - u\|_{h,*} \|\Pi_h u - u_h\|_h. \end{aligned}$$

We insert this estimate in the triangle inequality above, use the interpolation error estimates (3.33) and (3.34), and obtain

$$\begin{aligned} \|u - u_h\|_h &\leq \|u - \Pi_h u\|_h + \frac{\mu_b}{\mu_a} \|\Pi_h u - u\|_{h,*} \\ &\leq c_2 \left(\sum_{E \in \mathcal{T}_h} h_E^{2(s-1)} |u|_{H^s(E)}^2 \right)^{1/2} + c_3 \frac{\mu_b}{\mu_a} \left(\sum_{E \in \mathcal{T}_h} h_E^{2(s-1)} |u|_{H^s(E)}^2 \right)^{1/2} \\ &\leq (c_2 + c_3 \frac{\mu_b}{\mu_a}) \left(\sum_{E \in \mathcal{T}_h} h_E^{2(s-1)} |u|_{H^s(E)}^2 \right)^{1/2}, \end{aligned}$$

which proves the estimate (3.35) with $c = c_2 + c_3(\mu_b/\mu_a)$. \square

Now we proceed with solving the discrete variational problem (3.11) that is nothing but a huge system of linear algebraic equations. Indeed, let $\{p^{(i)} : i \in \mathcal{I}_h\}$ be some basis of V_{0h} , where \mathcal{I}_h is some index set, which we will specify later. Then we can express the approximate solution u_h in terms of this basis, i.e. $u_h(x, t) = \sum_{i \in \mathcal{I}_h} u_i p^{(i)}(x, t)$. Furthermore, each basis function is a valid test function. Thus, we obtain N_h equations from (3.11),

$$a_h(u_h, p^{(i)}) = l_h(p^{(i)}), \quad \text{for all } i \in \mathcal{I}_h, \quad (3.37)$$

where $N_h = |\mathcal{I}_h|$ is the dimension of V_{0h} . Now we replace u_h by its basis representation, which yields

$$\sum_{j \in \mathcal{I}_h} u_j \underbrace{a_h(p^{(j)}, p^{(i)})}_{=: (K_{ij})} = \underbrace{l_h(p^{(i)})}_{=: (f_i)}, \text{ for all } i \in \mathcal{I}_h. \quad (3.38)$$

We can rewrite this system in terms of a system of linear algebraic equations

$$\mathbf{K}_h \mathbf{u}_h = \mathbf{f}_h, \quad (3.39)$$

where $\mathbf{K}_h = (K_{ij})$, $\mathbf{u}_h = (u_i)$ and $\mathbf{f}_h = (f_i)$. The system matrix is non-symmetric, but positive definite due to Lemma 14. Indeed,

$$(\mathbf{K}_h \mathbf{v}_h, \mathbf{v}_h) = a_h(v_h, v_h) \geq \mu_a \|v_h\|_h^2 > 0 \quad (3.40)$$

for all $V_{0h} \ni v_h \leftrightarrow \mathbf{v}_h \in \mathbb{R}^{N_h} : \mathbf{v}_h \neq 0$. The linear system (3.39) can be solved efficiently and most important in parallel by either a sparse direct solver (e.g. sparse LU-factorisation) or an iterative solver (e.g., preconditioned GMRES). But how to construct such a basis $\{p^{(i)}\}$ of V_{0h} ? We need again the regular triangulation \mathcal{T}_h of our space-time domain \mathcal{Q} , which we already introduced in (3.1). We now define *shape functions* and the corresponding function set $\mathcal{F}(E)$. This function set is either a subspace or equal to the following function spaces

$$\begin{aligned} \mathbb{P}_k &:= \left\{ \sum_{|\alpha| \leq k} c_\alpha x^\alpha : c_\alpha \in \mathbb{R} \right\}, \\ \mathbb{Q}_k &:= \left\{ \sum_{\alpha_i \leq k} c_\alpha x^\alpha : i = 1, \dots, d+1, c_\alpha \in \mathbb{R} \right\}. \end{aligned}$$

Furthermore, we need some degrees of freedom, denoted by $l^{(E, \alpha)}$, which are functionals in the dual space $\mathcal{F}(E)^*$ of $\mathcal{F}(E)$. If these functionals span the whole dual space, i.e. they are a basis, or, equivalently, have the interpolation property

$$l^{(E, \alpha)}(v) = c_\alpha, \text{ for } v \in \mathcal{F}(E),$$

then we can uniquely determine all coefficients of $v \in \mathcal{F}(E)$ on an element E . In particular, we choose the point evaluations as our degrees of freedom, i.e., let $v \in \mathcal{F}(E)$, then

$$l^{(E, \alpha)}(v) = v(x^{(E, \alpha)}), \alpha \in \mathcal{A}_E, \quad (3.41)$$

where $x^{(E,\alpha)} \in E$ is called node and \mathcal{A}_E is a set of local indices. With this triple $(E, \mathcal{F}(E), \{l^{(E,\alpha)}\})$, which is called a *finite element*, we now define a local nodal basis of shape functions, i.e.,

$$\{p^{(E,\alpha)} : p^{(E,\alpha)} \in \mathcal{F}(E), \alpha \in \mathcal{A}_E\}, \quad (3.42)$$

with the property $l^{(E,\alpha)}(p^{(E,\beta)}) = \delta_{\alpha\beta}$.

Now we can define a global set of nodes $\{x^{(i)} : i \in \mathcal{I}_h\}$, and if $x^{(i)} \in \bar{E}$, then $x^{(i)} = x^{(E,\alpha)}$ for some α . Furthermore, we need a global set of degrees of freedom $\{l^{(i)} : i \in \mathcal{I}_h\}$, where $l^{(i)} = l^{(E,\alpha)}$ on E , and a global nodal basis $\{p^{(i)} : i \in \mathcal{I}_h\}$, with $l^{(i)}(p^{(j)}) = \delta_{ij}$ and $p^{(i)} = p^{(E,\alpha)}$ on E . Then this global nodal basis spans our discrete function space $V_{0h} = \text{span}\{p^{(i)} : i \in \mathcal{I}_h\}$.

From now on, we restrict ourselves to triangular elements E and the polynomial space \mathbb{P}_1 . Hence, we have three degrees of freedom for $p^{(i)} \in \mathbb{P}_1$, which we will determine by point evaluation in the three corner points of the triangle E . To efficiently compute the entries in \mathbf{K}_h and \mathbf{f}_h , we observe that the nodal basis functions $p^{(i)}$ have only local support, which will result in a sparse matrix \mathbf{K}_h . Therefore, we can write each entry as

$$\begin{aligned} (\mathbf{K}_h)_{ij} &= \begin{cases} 0, & \text{if } B_{ij} = B_i \cap B_j = \emptyset, \\ \sum_{E \in B_{ij}} a_{h,e}(p^{(j)}, p^{(i)}), & \text{else} \end{cases}, \\ (\mathbf{f}_h)_i &= \sum_{E \in B_i} l_{h,e}(p^{(i)}), \end{aligned}$$

where $B_i = \{E \in \mathcal{T}_h : x^{(i)} \in \bar{E}\}$ is the neighbourhood of a node $x^{(i)}$ and

$$\begin{aligned} a_{h,e}(u_h, v_h) &:= \int_E \partial_t u_h v_h + \theta_E h_E \partial_t u_h \partial_t v_h \, d(x, t) \\ &\quad + \int_E \nu \nabla_x u_h \cdot \nabla_x v_h + \theta_E h_E \nu \nabla_x u_h \cdot \nabla_x (\partial_t v_h) \, d(x, t) \end{aligned} \quad (3.43)$$

$$\begin{aligned} &\quad - \int_{\partial E} \theta_E h_E \nu \nabla_x u_h \cdot \vec{n}_x v_h \, ds_{(x,t)}, \\ l_{h,e}(v_h) &:= \int_E f(v_h + \theta_E h_E \partial_t v_h) \, d(x, t), \end{aligned} \quad (3.44)$$

are the integrals over one element.

In order to compute the entries of \mathbf{K}_h , we will assemble the stiffness matrix \mathbf{K}_h and the load vector \mathbf{f}_h element-wise, i.e., on each element E , we have to identify $i \leftrightarrow \alpha$ and $j \leftrightarrow \beta$, so we obtain the local element matrix $\mathbf{K}_h^{(E)}$ and the element load vector $\mathbf{f}_h^{(E)}$, with

$$(\mathbf{K}_h^{(E)})_{\alpha\beta} = a_{h,e}(p^{(E,\beta)}, p^{(E,\alpha)}), \quad \text{and} \quad (\mathbf{f}_h^{(E)})_\alpha = l_{h,e}(p^{(E,\alpha)}).$$

In order to avoid the computation of the coefficients of $p^{(E,\alpha)}$ on each element, we will instead transform the arbitrary triangle E to a canonical triangle, the so called *reference triangle* Δ , with

$$\Delta := \{(\xi_1, \xi_2) : \xi_1 + \xi_2 \leq 1 \wedge \xi_1, \xi_2 \geq 0\}.$$

For our finite elements, it is sufficient to do this transformation via an affine mapping X_E , which is defined as

$$\xi \mapsto X_E(\xi) := x^{(E,1)} + \underbrace{\begin{pmatrix} x_1^{(E,2)} - x_1^{(E,1)} & x_1^{(E,3)} - x_1^{(E,1)} \\ x_1^{(E,2)} - x_2^{(E,1)} & x_2^{(E,3)} - x_2^{(E,1)} \end{pmatrix}}_{J_E} \xi.$$

On the reference triangle Δ , the shape functions $p^{(\alpha)}$ can be easily computed, i.e.,

$$p^{(1)}(\xi) = 1 - \xi_1 - \xi_2, \quad p^{(2)} = \xi_1, \quad \text{and} \quad p^{(3)} = \xi_2.$$

We then obtain the shape functions on an arbitrary element E via the inverse mapping X_E^{-1} , i.e.,

$$p^{(E,\alpha)} = p^{(\alpha)} \circ X_E^{-1}. \quad (3.45)$$

Hence, we can compute the element matrices $\mathbf{K}_h^{(E)}$ and element load vectors $\mathbf{f}_h^{(E)}$ by transforming the integrals to the reference element Δ . The transformed integrals can now be approximated by some quadrature rule. In particular, we used the first three point rule from [23, Table 4.1]. If we now perform these calculations for each element E , and add the entries of $\mathbf{K}_h^{(E)}$ and $\mathbf{f}_h^{(E)}$ to the corresponding entries of \mathbf{K}_h and \mathbf{f}_h , respectively, we have fully assembled our linear system (3.39). Note that as our bilinear form $a_h(\cdot, \cdot)$ is non-symmetric, the stiffness matrix \mathbf{K}_h is also non-symmetric. However, so far, we do not have incorporated the initial- and boundary-conditions. First of all, we deduce that the initial condition (1.3) can be seen as a Dirichlet boundary condition for the space time cylinder \mathcal{Q} . Since we consider only homogeneous initial and boundary values, this incorporation can be easily achieved. We first identify all vertices which are on the Dirichlet boundary. Let us denote the set of indices of such vertices by \bar{I}_h . Then, for each $i \in \bar{I}_h$, we set

$$f_i = 0, \quad K_{ij} = 0 \text{ for } j \in \bar{I}_h \setminus \{i\}, \quad \text{and} \quad K_{ii} = 1.$$

For further details on the incorporation of boundary conditions, we refer to e.g. [10].

4 Implementation

To validate our theoretical results from Section 3, we performed some numerical experiments. Let $\Omega := (0, 1)$ and $\mathcal{Q} := \Omega \times (0, 1) = (0, 1)^2$. We want to solve the initial boundary value problem (1.1)-(1.3) with homogeneous boundary and initial conditions,

$$\partial_t u(x, t) - \partial_x(\nu(x, t)\partial_x u(x, t)) = f(x, t), \quad (x, t) \in (0, 1)^2, \quad (4.1)$$

$$u(x, 0) = 0, \quad x \in [0, 1], \quad (4.2)$$

$$u(0, t) = u(1, t) = 0, \quad t \in (0, 1), \quad (4.3)$$

and ν being piecewise positive constant, and

$$f(x, t) := \pi \sin(\pi x) (\cos(\pi t) + \pi \sin(\pi x)).$$

For the case $\nu \equiv 1$, we know that the exact solution is

$$u(x, t) = \sin(\pi x) \sin(\pi t). \quad (4.4)$$

Thus, for this case, we can easily compute convergence rates. But if ν has jumps, we do not know the exact solution. Hence, we have to replace the exact solution by an approximate solution computed on a fine grid, see Section 5 for details.

The FEM was implemented in our C++ code *SpaceTimeFEM++*. The linear system (3.39) was solved by means of the direct solver PARDISO 5.0.0, see [11]. Until now, the PARDISO solver for non-symmetric matrices is only parallelized by the use of OpenMP (shared memory) instead of MPI (distributed memory).

5 Numerical Results

The numerical experiments presented in this section were performed on the RADON1¹ high performance computing cluster at RICAM, Linz. Due to the nature of our linear system and the used solver, we could not use the full potential of the hardware. The initial meshing was done with NETGEN (see [20]) and the finer meshes were obtained by a subsequent uniform refinement procedure. We measured the absolute error in both the L_2 - and the mesh-dependent norm (3.12), i.e., we computed $\|u - u_h\|_{L_2(\mathcal{Q})}$ and $\|u - u_h\|_h$, where u and u_h denote the exact and approximate solutions, respectively. In each graph, we also include the expected convergence rate, i.e., $\mathcal{O}(h^p)$ for the mesh-dependent norm (3.12) and $\mathcal{O}(h^{p+1})$ for the L_2 -norm.

¹<https://www.ricam.oeaw.ac.at/hpc/>

5.1 Constant θ_E

For the experiments in this section, we will choose a $\theta_E = \theta$ and perform a series of uniform refinements without changing the θ_E . Moreover, for this subsection, we restrict ourselves to linear basis functions, i.e., $p = 1$. Thus, we expect convergence rates of $\mathcal{O}(h)$ for the mesh-dependent norm (3.12) and $\mathcal{O}(h^2)$ for the L_2 -norm, provided that our solution has high enough regularity. Furthermore, we expect that the convergence rates for the $\|\cdot\|_h$ -norm are not influenced by θ .

5.1.1 Constant coefficient case

For our first test case, let $\nu(x, t) \equiv 1$, $\forall(x, t) \in \mathcal{Q}$, and let the exact solution be given by

$$u(x, t) = \sin(\pi x) \sin(\pi t). \quad (5.1)$$

The coarsest mesh has 132 degrees of freedom (dofs), see Fig. 1, whereas the finest one has 29 108 225 dofs.

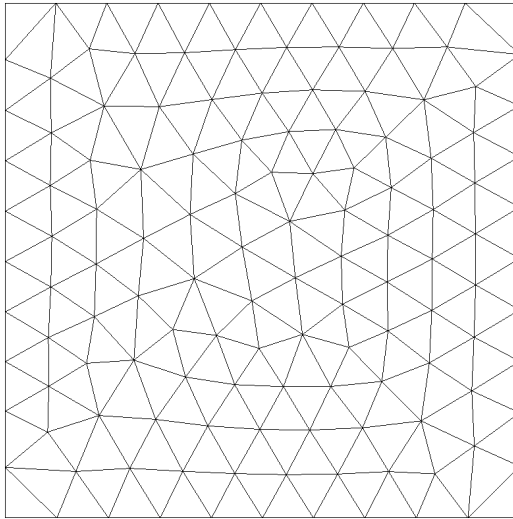


Figure 1: Initial mesh with 132 vertices.

We can see in Fig. 2 that θ directly influences the convergence rates in the L_2 -norm, with linear convergence for $\theta = 0.1$ and almost quadratic convergence for $\theta = 10^{-5}$. The same does not hold for the mesh-dependent norm $\|\cdot\|_h$, as we can see in Fig. 3. Instead, we observe almost no change in both the absolute error and the convergence rate. But what if we examine the parts of the $\|\cdot\|_h$ -norm separately? For the spatial derivative part, we observe that it matches the behaviour of the full norm. The L_2 -norm of the

error on the top of the space-time cylinder matches the behaviour of the full L_2 -norm. However, for the temporal derivative part, we only get reduced convergence rates, c.f. Fig. 4. This is due to the scaling wrt the mesh-size h_E in front of the term.

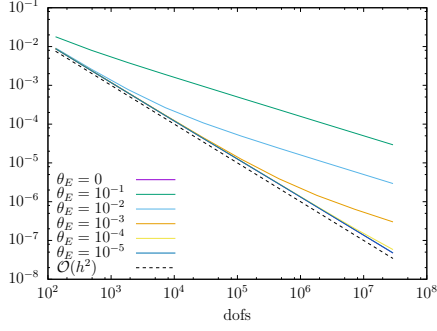


Figure 2: This plot shows the influence of θ_E on the L_2 -norm for $\nu \equiv 1$.

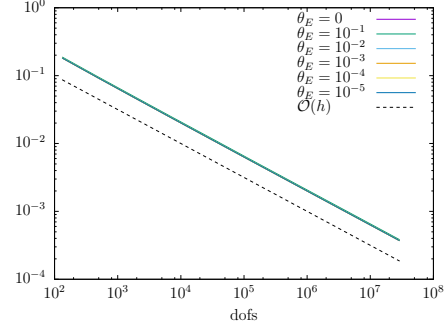


Figure 3: This plot shows the influence of θ_E on the $\|\cdot\|_h$ -norm for $\nu \equiv 1$.

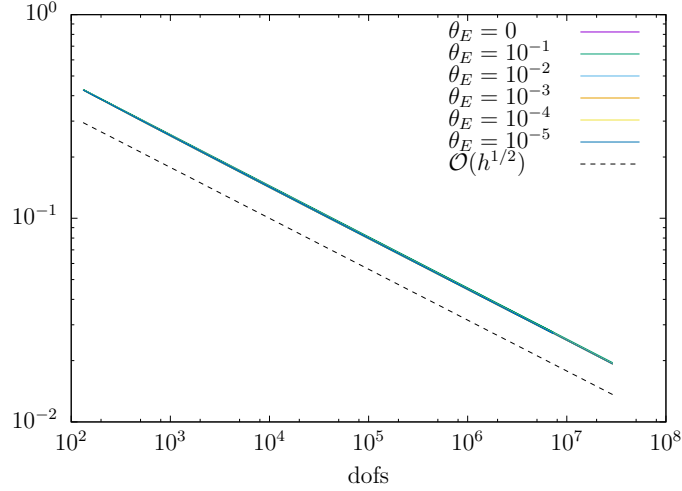


Figure 4: This plot shows the influence of θ_E on $\|\partial_t(u-u_h)\|_{L_2(\mathcal{Q})}$ in the $\|\cdot\|_h$ -norm for $\nu \equiv 1$.

5.1.2 Jumps only in space

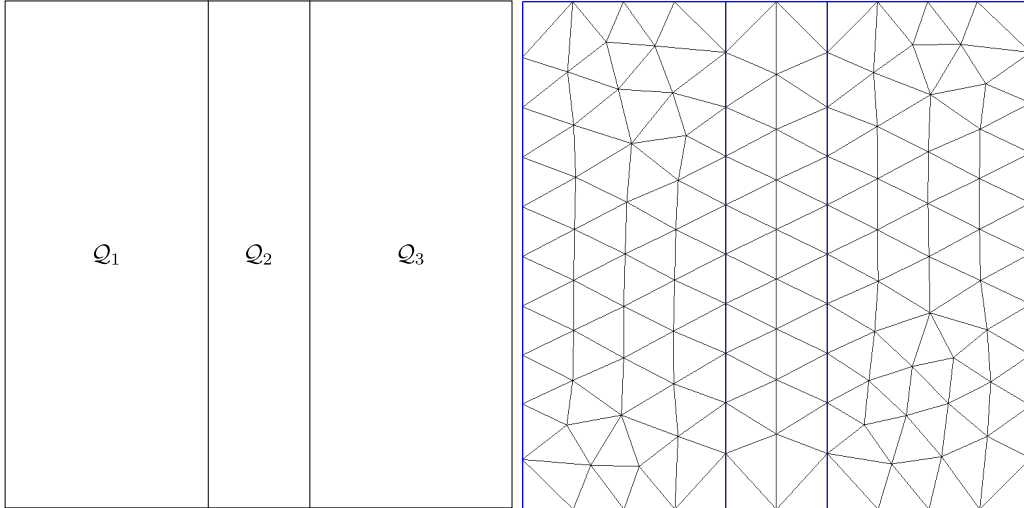


Figure 5: A sketch of the domain with jumps only in space and the initial mesh.

In our second test case, we now allow a jumping coefficient ν , but restrict this jumps to be only in space, as illustrated in Fig. 5. Therefore, ν is defined as

$$\nu(x, t) := \begin{cases} \nu_1, & \text{for } (x, t) \in \mathcal{Q}_1 \cup \mathcal{Q}_3, \\ \nu_2, & \text{for } (x, t) \in \mathcal{Q}_2. \end{cases}$$

Due to this discontinuity, we do not know the exact solution. Instead we choose the solution on a very fine mesh as our new "exact" solution and compared it against the solutions on the coarser meshes. As a consequence, we have to treat the obtained convergence rates with caution, as the coarser solutions naturally converge to the finest solution. We can observe this effect directly in the following plots, as all of them will have steeper descent for the highest number of dofs. The coarsest computational domain consists of 121 vertices and the mesh for the "exact" solution has 26 224 146 dofs. The finest mesh for which we obtain convergence rates has 6 558 711 dofs in total. For the values of ν_1 and ν_2 , we always chose $\nu_1 = 1$ and $\nu_2 \in \{10, 100, 1000\}$. We start with $\nu_2 = 10$. In Fig. 6 and Fig. 7, we observe a different behaviour as in the uniform case. For a discontinuous ν , we observe that θ now has influence on the absolute error in the $\|\cdot\|_h$ -norm. Furthermore, any value of θ less than $\theta = 0.01$ yields almost the same convergence rates for both the L_2 - and the $\|\cdot\|_h$ -norm. However, a possible reason for this might be that our number of dofs is just not high enough (see Section 6), because if we compare the plot for $\theta = 0.01$ in Fig. 2 with the one in Fig. 6, they seem to

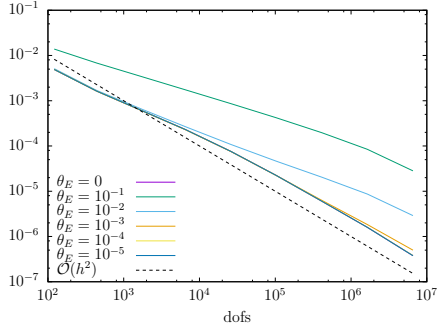


Figure 6: This plot shows the influence of θ_E on the L_2 -norm for $\nu_2 = 10$.

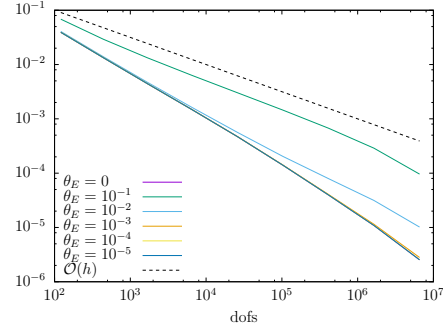


Figure 7: This plot shows the influence of θ_E on the $\|\cdot\|_h$ -norm for $\nu_2 = 10$.

have a similar behaviour.

If we increase the height of the discontinuity by a factor of 10, i.e., $\nu_2 = 100$,

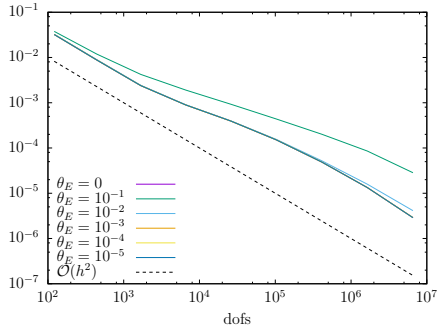


Figure 8: This plot shows the influence of θ_E on the L_2 -norm for $\nu_2 = 100$.

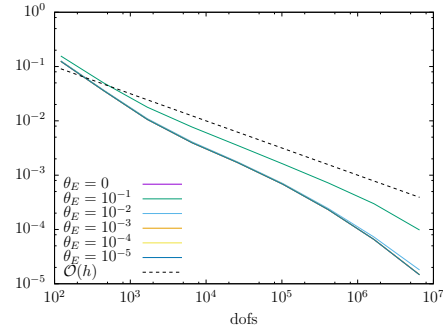


Figure 9: This plot shows the influence of θ_E on the $\|\cdot\|_h$ -norm for $\nu_2 = 100$.

we observe in Fig. 8 and Fig. 9, that the values smaller than $\theta = 0.1$ yield almost the same convergence rates as the limit case $\theta = 0$.

This effect is even stronger if we increase the jump height once again by a factor of 10. For $\nu_2 = 1000$, the parameter θ has even less influence on both norms than before, as you can observe in Fig. 10 and Fig. 11.

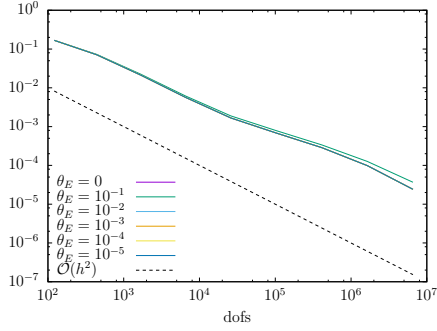


Figure 10: This plot shows the influence of θ_E on the L_2 -norm for $\nu_2 = 1000$.

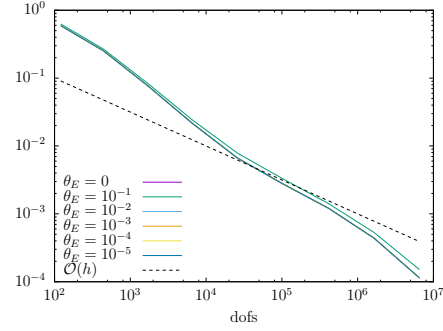


Figure 11: This plot shows the influence of θ_E on the $\|\cdot\|_h$ -norm for $\nu_2 = 1000$.

5.1.3 Jumps in space and time

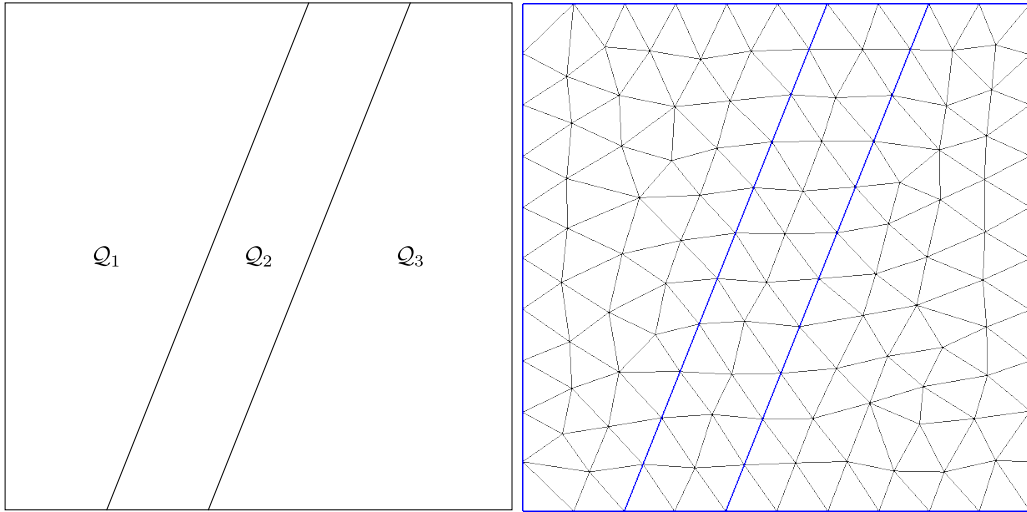


Figure 12: A sketch of the domain with jumps both in space and time and the corresponding initial mesh.

For our third test case, the jumps happen not only in space, but also in time, as illustrated in Fig. 12. Again, we define ν as

$$\nu(x, t) = \begin{cases} \nu_1, & \text{for } (x, t) \in \mathcal{Q}_1 \cup \mathcal{Q}_3, \\ \nu_2, & \text{for } (x, t) \in \mathcal{Q}_2. \end{cases}$$

As in the second test case, we do not know a exact solution. Hence, we obtain error behaviour and convergence rates as before. The choice of the diffusion coefficient ν remains almost the same, i.e., $\nu_1 = 1$ and $\nu_2 \in \{10, 100, 1000, 4000\}$.

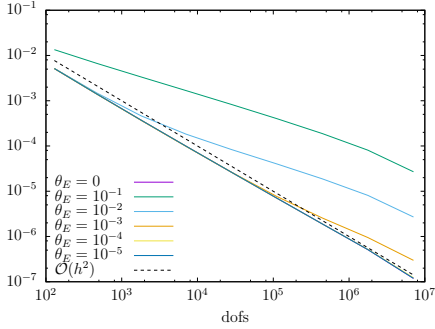


Figure 13: This plot shows the influence of θ_E on the L_2 -norm for $\nu_2 = 10$.

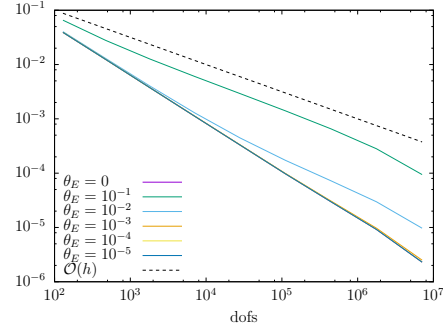


Figure 14: This plot shows the influence of θ_E on the $\|\cdot\|_h$ -norm for $\nu_2 = 10$.

We start again with $\nu_2 = 10$ and observe that θ has more influence than in the second test case, c.f. Fig. 6 and Fig. 13. Moreover, if we compare it with the L_2 -plot of the uniform case, we observe a very similar behaviour. For the $\|\cdot\|_h$ -norm, θ has again direct influence and the plot has analogous behaviour as before (see Fig. 14). We continue with $\nu_2 = 100$. Here, the plot

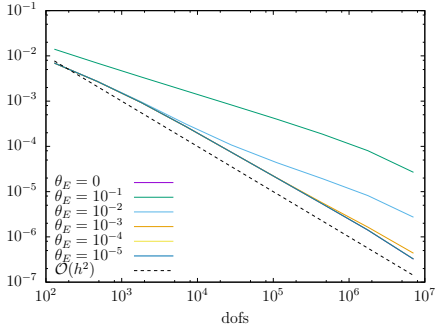


Figure 15: This plot shows the influence of θ_E on the L_2 -norm for $\nu_2 = 100$.

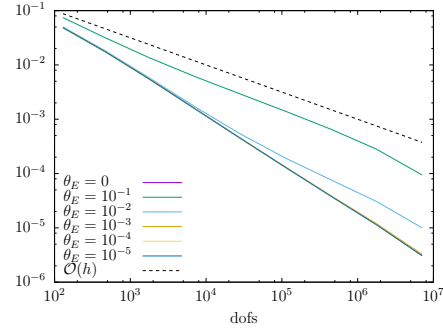


Figure 16: This plot shows the influence of θ_E on the $\|\cdot\|_h$ -norm for $\nu_2 = 100$.

of the L_2 -norm has much similarity to the second test case with $\nu_2 = 10$. The same holds for the $\|\cdot\|_h$ -norm. For this geometry, θ seems to have much more influence on the error rates as in second test case. We can observe this for $\nu_2 = 1000$, as the error rates for $\theta = 0.1$ is still distinguishable from the other θ s and, for a high number of dofs, this difference is very clear, as we can see in Fig. 17 and Fig. 18. So what happens if we increase the height of the discontinuity once again? Let now $\nu_2 = 4000$. Then, our parameter θ has little to no influence on the absolute error. Only for the highest number of vertices, we can clearly distinguish between $\theta = 0.1$ and the smaller θ s (see Fig. 19 and Fig. 20).

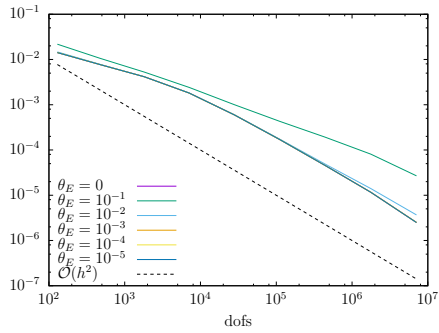


Figure 17: This plot shows the influence of θ_E on the L_2 -norm for $\nu_2 = 1000$.

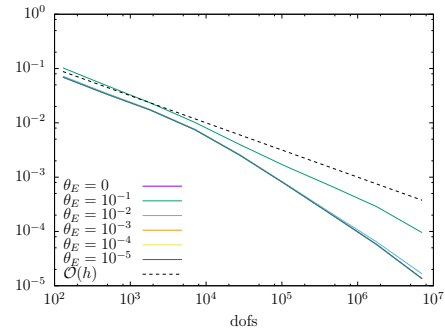


Figure 18: This plot shows the influence of θ_E on the $\|\cdot\|_h$ -norm for $\nu_2 = 1000$.

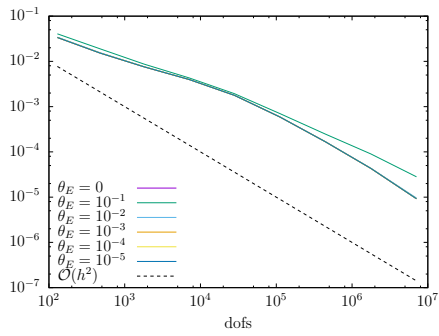


Figure 19: This plot shows the influence of θ_E on the L_2 -norm for $\nu_2 = 4000$.

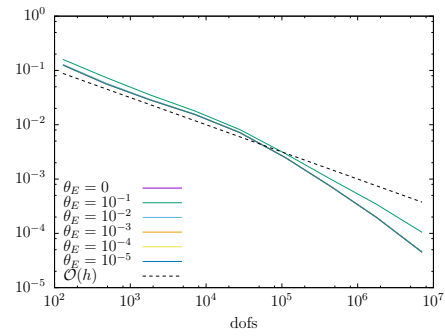


Figure 20: This plot shows the influence of θ_E on the $\|\cdot\|_h$ -norm for $\nu_2 = 4000$.

5.1.4 Jumps in space and time with change of direction

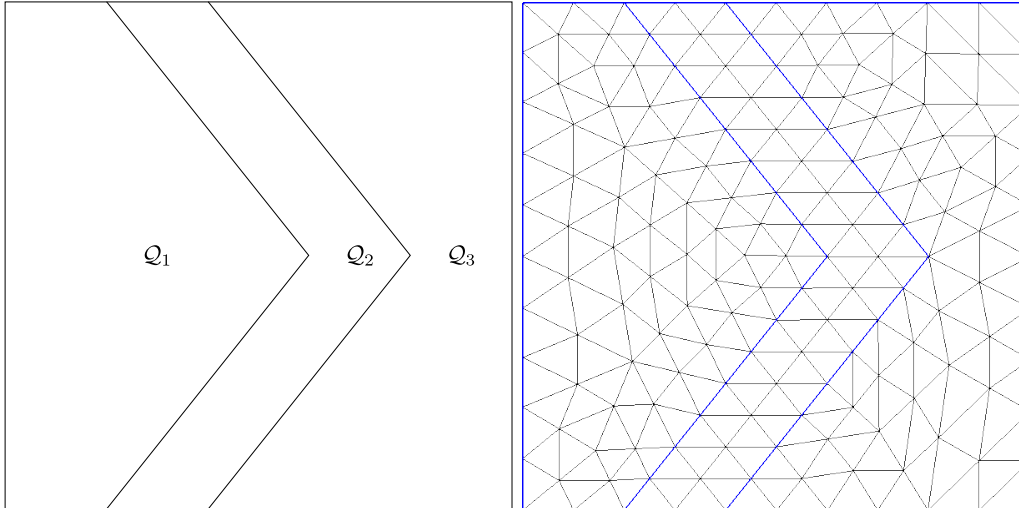


Figure 21: A sketch of the domain with jumps both in space and time and a change in direction and the initial mesh.

For the fourth and last test case, we allow now domains where the discontinuity changes its direction, as in Fig. 21. This is typically for the case of a so-called line motor. We use the same definition for ν as before, i.e.,

$$\nu(x, t) = \begin{cases} \nu_1, & \text{for } (x, t) \in \mathcal{Q}_1 \cup \mathcal{Q}_3, \\ \nu_2, & \text{for } (x, t) \in \mathcal{Q}_2. \end{cases}$$

The exact solution is again not available, hence we use the same procedure for convergence rates as in the second and third test case. The values for ν_1 and ν_2 remain $\nu_1 = 1$ and $\nu_2 \in \{10, 100, 1000\}$. The initial mesh consists of 165 vertices, the mesh for our "exact" solution has 37758977 dofs and the last solution for which we obtain convergence rates has 9442305 vertices.

Now let $\nu_2 = 10$. In contrast to the previous two test cases, we observe an significant difference in the behaviour of the L_2 - and $\|\cdot\|_h$ -norm (compare Fig. 22 and Fig. 23). For the L_2 -norm, we observe that for all the θ less than $\theta = 0.01$, the errors have little difference, while the error for $\theta = 0.1$ is greater. The $\|\cdot\|_h$ -norm behaves interestingly, as for the coarsest mesh, we can differ between $\theta = 0.1$ and $\theta \leq 0.01$, but as the meshes become finer, all plot lines merge and then the difference is almost negligible. For higher discontinuities, i.e. $\nu_2 \in \{100, 1000\}$, the error behaves exactly in the same manner, so ν seems to have very little influence for this type of geometry.

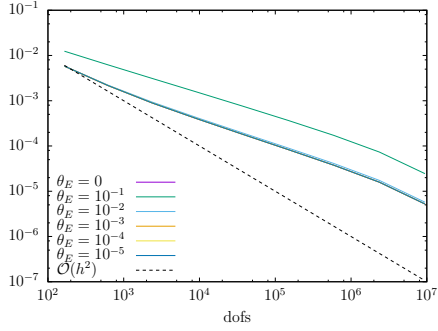


Figure 22: This plot shows the influence of θ_E on the L_2 -norm for $\nu_2 = 10$.

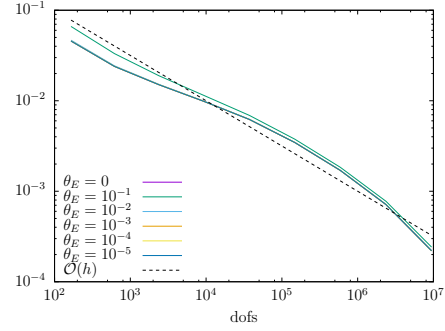


Figure 23: This plot shows the influence of θ_E on the $\|\cdot\|_h$ -norm for $\nu_2 = 10$.

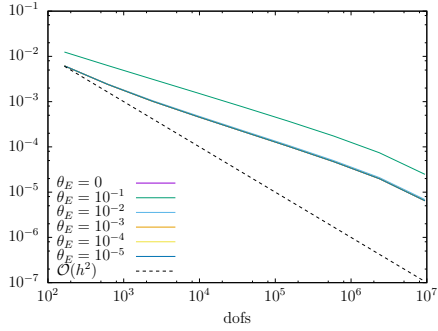


Figure 24: This plot shows the influence of θ_E on the L_2 -norm for $\nu_2 = 10$.

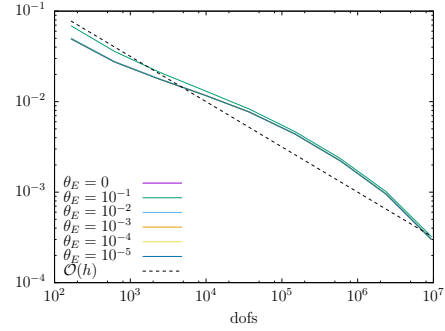


Figure 25: This plot shows the influence of θ_E on the $\|\cdot\|_h$ -norm for $\nu_2 = 100$.

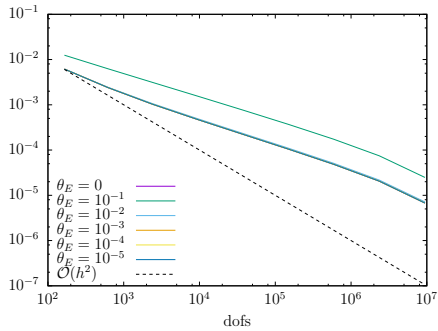


Figure 26: This plot shows the influence of θ_E on the L_2 -norm for $\nu_2 = 1000$.

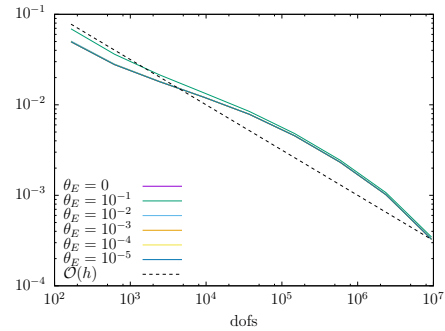


Figure 27: This plot shows the influence of θ_E on the $\|\cdot\|_h$ -norm for $\nu_2 = 1000$.

5.2 Variable θ_E

For the experiments in this section, we now allow different θ_E for each element. In particular, we test for the case $\theta_E = h_E$, for all $E \in \mathcal{T}_h$ to validate our theoretical results. As we have seen from the experiments in the previous section, in the case of linear shape functions, i.e., $p = 1$, the influence of θ_E on the convergence rates is almost negligible. Therefore we performed the same four experiments as in the section before, but also with quadratic shape functions, i.e., $p = 2$.

5.2.1 Constant coefficient case

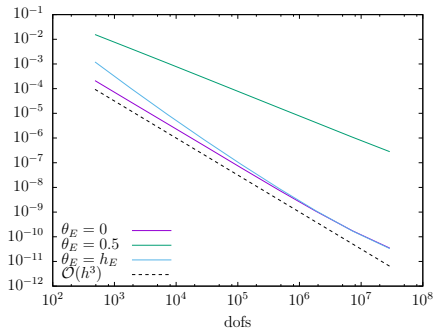


Figure 28: This plot shows the influence of θ_E on the L_2 -norm for $\nu \equiv 1$.

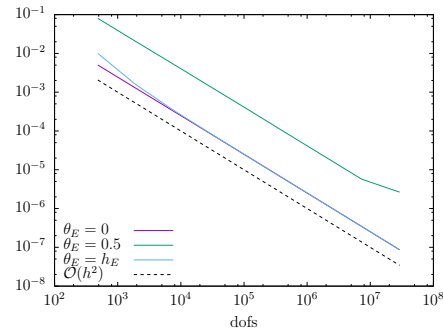


Figure 29: This plot shows the influence of θ_E on the $\|\cdot\|_h$ -norm for $\nu \equiv 1$.

For the constant coefficient case, we immediately observe that the choice $\theta_E = \mathcal{O}(h_E)$ is crucial in order to obtain optimal rates, i.e., $\mathcal{O}(h^2)$ for the mesh-dependent norm (3.12), and $\mathcal{O}(h^3)$ for the L_2 -norm, c.f. Fig. 28 and 29.

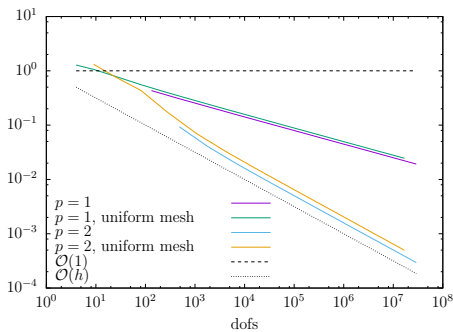


Figure 30: This plot shows the influence of $\theta_E = h_E$ on $\|\partial_t(u - u_h)\|_{L_2(\mathcal{Q})}$ in the $\|\cdot\|_h$ -norm for $\nu \equiv 1$.

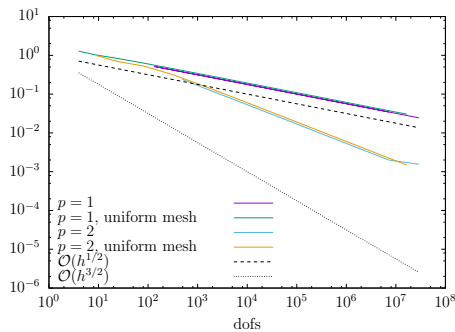


Figure 31: This plot shows the influence of $\theta_E = 0.5$ on $\|\partial_t(u - u_h)\|_{L_2(\mathcal{Q})}$ in the $\|\cdot\|_h$ -norm for $\nu \equiv 1$.

We again examined the temporal part $\|\partial_t(u - u_h)\|_{L_2(\mathcal{Q})}$ separately, comparing our almost uniform mesh with a real uniform mesh, i.e., $h_E = h$ for all $E \in \mathcal{T}_h$. Moreover, we also included the rates for linear shape functions ($p = 1$). For $\theta_E = h_E$, we observe that for $p = 1$, the actual rates are better than expected, whereas for $p = 2$, the results confirm the theory (c.f. Fig. 30). For a fixed $\theta_E = 0.5$ however, the rates for $p = 1$ validate the theory, but for $p = 2$, the observed rates are worse than the predicted ones, c.f. Fig. 31.

5.2.2 Jumps only in space

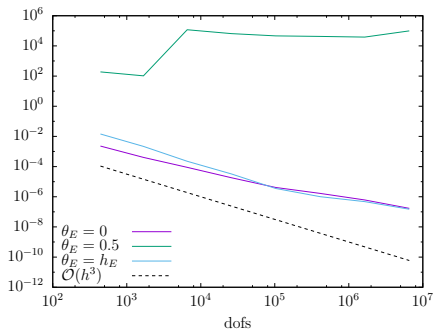


Figure 32: This plot shows the influence of θ_E on the L_2 -norm for $\nu_2 = 1000$.

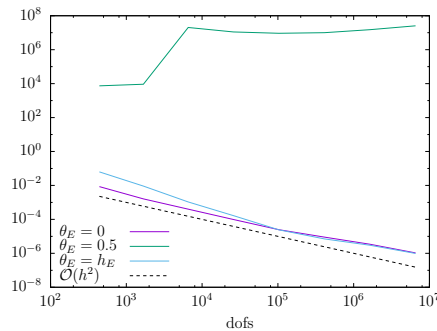


Figure 33: This plot shows the influence of θ_E on the $\|\cdot\|_h$ -norm for $\nu_2 = 1000$.

For the second experiment, we now have a diffusion coefficient which does depend on the spatial variable, i.e.,

$$\nu = \begin{cases} 1, & \text{for } x \in (0, 0.4) \cup (0.6, 1), \\ 1000, & \text{else.} \end{cases}$$

In this case, we see that the scheme is even more susceptible to the choice of θ_E . If we compare the rates with the constant coefficient case, we note that for $\theta_E = 0.5$ for all $E \in \mathcal{T}_h$, we do not get any convergence, c.f. Fig. 32 and 33. Additionally, we do not get optimal rates even for $\theta_E = h_E$, which is most likely due to a loss in regularity of the solution.

5.2.3 Jumps in space and time

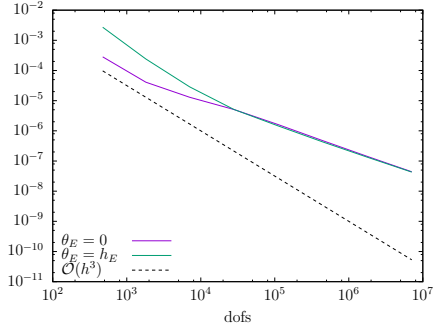


Figure 34: This plot shows the influence of θ_E on the L_2 -norm for $\nu_2 = 1000$.

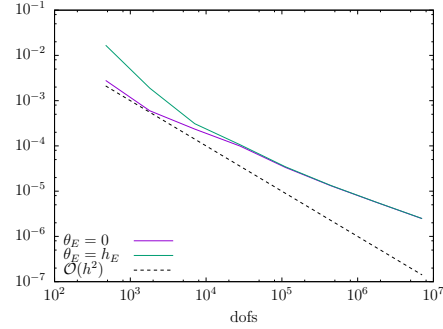


Figure 35: This plot shows the influence of θ_E on the $\|\cdot\|_h$ -norm for $\nu_2 = 1000$.

If we now admit that the discontinuity also depends on t , i.e.,

$$\nu(x, t) = \begin{cases} 1, & \text{for } (x, t) \in \mathcal{Q}_1 \cup \mathcal{Q}_3, \\ 1000, & \text{for } (x, t) \in \mathcal{Q}_2, \end{cases}$$

the effect of a fixed θ_E becomes even worse. The magnitude of the absolute errors is now of order 10^{40} . Hence, we excluded this choice of θ_E in the plots. As in the previous case, we lose the optimal rates, even for $\theta_E = 0$, c.f. Fig. 36 and 37.

5.2.4 Jumps in space and time with change of direction

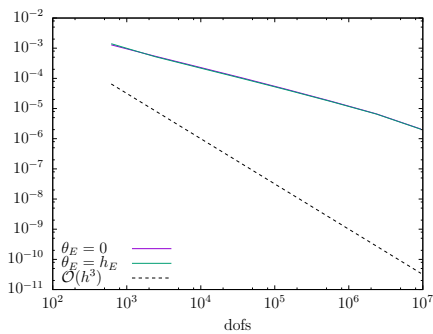


Figure 36: This plot shows the influence of θ_E on the L_2 -norm for $\nu_2 = 1000$.

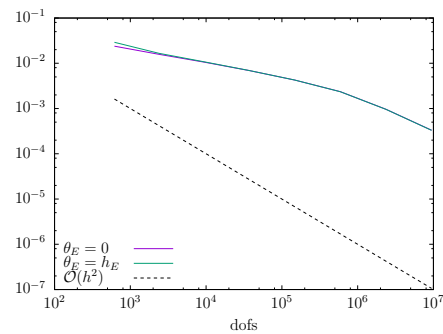


Figure 37: This plot shows the influence of θ_E on the $\|\cdot\|_h$ -norm for $\nu_2 = 1000$.

In the last test case, where the lines of discontinuity change their direction, we again excluded the plots for $\theta_E = 0.5$ for all $E \in \mathcal{T}_h$, as the magnitude was

to high. As for the convergence rates for $\theta_E = h_E$ and $\theta_E = 0$, we observe that in both cases, we lose the full convergence rates, c.f. Fig. 36 and 37 due to the reduced regularity of the solution.

6 Conclusions and Future Work

In this paper, following [12], we first showed that the parabolic initial boundary value problem (1.1)-(1.3) has a unique, generalized solution in $\dot{H}^{1,0}(\mathcal{Q})$, that even belongs to $\dot{V}_2^{1,0}(\mathcal{Q})$. We proceeded by deriving a stable space-time finite element scheme (3.8), for which we showed coercivity (ellipticity) and boundedness, as well as an a priori error estimate with optimal rates. However, these optimal rates come with a price, i.e., we have to choose $\theta_E = \mathcal{O}(h_E)$ for all $E \in \mathcal{T}_h$. We performed a numerical experiment for $\mathcal{Q} = (0,1)^2$ and a constant diffusion coefficient $\nu = \text{const} > 0$, with a highly smooth solution. More numerical experiments were performed for a discontinuous diffusion coefficient. All numerical experiments yielded the expected results.

In future work, we could try to derive some a priori error-estimate for the L_2 -norm, which was always studied numerically in our experiments in Section 5. Moreover, one could develop an a posteriori error estimator, which would enable us to use adaptive mesh refinement, leading to a space-time Adaptive Finite Element Method (AFEM). We mention that our scheme is prepared for AFEM, since we allow local mesh-sizes h_E for $E \in \mathcal{T}_h$ under the condition of shape regularity of the element E . This will help in analysing problems with a discontinuous diffusion coefficient ν . Then we can improve the solver for the huge algebraic linear system. We can switch from a sparse direct solver to a AMG-preconditioned GMRES-method, as was done in [14], which would enable us to reach a higher number of dofs, as well as the treatment of 2D and even 3D problems. We can then combine the space-time AFEM with Nested Iterations, which drastically reduces the solving time. The main future goal is the application to nonlinear parabolic problems and eddy current problems, which typically arise in electrical engineering.

References

- [1] BRAESS, D. *Finite Elemente; Theorie, schnelle Löser und Anwendungen in der Elastizitätstheorie*, 4., bearbeitete und erweiterte auflage ed. Springer-Verlag Berlin Heidelberg, Berlin, Heidelberg, 2007.
- [2] BRENNER, S. C., AND SCOTT, L. R. *The mathematical theory of finite element methods*, third ed., vol. 15 of *Texts in Applied Mathematics*. Springer, New York, 2008.
- [3] CIARLET, P. G. *The finite element method for elliptic problems*. North-Holland Publishing Co., Amsterdam-New York-Oxford, 1978. Studies in Mathematics and its Applications, Vol. 4.
- [4] DI PIETRO, D. A., AND ERN, A. *Mathematical aspects of discontinuous Galerkin methods*, vol. 69 of *Mathématiques & Applications (Berlin) [Mathematics & Applications]*. Springer, Heidelberg, 2012.
- [5] DUAN, H., LI, S., TAN, R. C. E., AND ZHENG, W. A delta-regularization finite element method for a double curl problem with divergence-free constraint. *SIAM J. Numer. Anal.* 50, 6 (2012), 3208–3230.
- [6] GANDER, M. J. 50 years of time parallel integration. In *Multiple Shooting and Time Domain Decomposition*. Springer Verlag, Heidelberg, Berlin, 2015, pp. 69–114.
- [7] HACKBUSCH, W. Parabolic multigrid methods. In *Computing methods in applied sciences and engineering, VI (Versailles, 1983)*. North-Holland, Amsterdam, 1984, pp. 189–197.
- [8] HEUSER, H. *Gewöhnliche Differentialgleichungen. Einführung in Lehre und Gebrauch.*, 4th revised ed. ed. Stuttgart: Teubner, 2004.
- [9] HUGHES, T. J. R., AND HULBERT, G. M. Space-time finite element methods for elastodynamics: formulations and error estimates. *Comput. Methods Appl. Mech. Engrg.* 66, 3 (1988), 339–363.
- [10] JUNG, M., AND LANGER, U. *Methode der finiten Elemente für Ingenieure - Eine Einführung in die numerischen Grundlagen und Computersimulation*. Springer-Verlag, Berlin Heidelberg New York, 2013.
- [11] KUZMIN, A., LUISIER, M., AND SCHENK, O. Fast methods for computing selected elements of the greens function in massively parallel

- nanoelectronic device simulations. In *Euro-Par 2013 Parallel Processing*, F. Wolf, B. Mohr, and D. Mey, Eds., vol. 8097 of *Lecture Notes in Computer Science*. Springer Berlin Heidelberg, 2013, pp. 533–544.
- [12] LADYŽHENSKAYA, O. A. *The boundary value problems of mathematical physics*, vol. 49 of *Applied Mathematical Sciences*. Springer-Verlag, New York, 1985. Translated from the Russian by Jack Lohwater [Arthur J. Lohwater].
- [13] LANG, J. *Adaptive multilevel solution of nonlinear parabolic PDE systems*, vol. 16 of *Lecture Notes in Computational Science and Engineering*. Springer-Verlag, Berlin, 2001. Theory, algorithm, and applications.
- [14] LANGER, U., MOORE, S. E., AND NEUMÜLLER, M. Space-time isogeometric analysis of parabolic evolution problems. *Comput. Methods Appl. Mech. Engrg.* 306 (2016), 342–363.
- [15] MOLLET, C. Stability of Petrov-Galerkin discretizations: application to the space-time weak formulation for parabolic evolution problems. *Comput. Methods Appl. Math.* 14, 2 (2014), 231–255.
- [16] MONT, A. D. *Adaptive unstructured spacetime meshing for four-dimensional spacetime discontinuous Galerkin finite element methods*. PhD thesis, University of Illinois at Urbana-Champaign, 2011.
- [17] NEUMÜLLER, M. *Space-time methods; fast solvers and applications*. Monographic series TU Graz : Computation in engineering and science ; 20. Verl. der Techn. Univ. Graz, Graz, 2013.
- [18] NEUMÜLLER, M., AND STEINBACH, O. Refinement of flexible space-time finite element meshes and discontinuous Galerkin methods. *Comput. Vis. Sci.* 14, 5 (2011), 189–205.
- [19] RIVIÈRE, B. *Discontinuous Galerkin methods for solving elliptic and parabolic equations*, vol. 35 of *Frontiers in Applied Mathematics*. Society for Industrial and Applied Mathematics (SIAM), Philadelphia, PA, 2008. Theory and implementation.
- [20] SCHÖBERL, J. NETGEN - An advancing front 2D/3D-mesh generator based on abstract rules. *Computing and Visualization in Science* 1 (1997), 41–52.
- [21] SCHWAB, C., AND STEVENSON, R. Space-time adaptive wavelet methods for parabolic evolution problems. *Math. Comp.* 78, 267 (2009), 1293–1318.

- [22] STEINBACH, O. Space-time finite element methods for parabolic problems. *Comput. Methods Appl. Math.* 15, 4 (2015), 551–566.
- [23] STRANG, G., AND FIX, G. J. *An analysis of the finite element method*. Prentice-Hall, Inc., Englewood Cliffs, N. J., 1973. Prentice-Hall Series in Automatic Computation.
- [24] THITE, S. Adaptive spacetime meshing for discontinuous Galerkin methods. *Comput. Geom.* 42, 1 (2009), 20–44.
- [25] THOMÉE, V. *Galerkin finite element methods for parabolic problems*, second ed., vol. 25 of *Springer Series in Computational Mathematics*. Springer-Verlag, Berlin, 2006.
- [26] TOULOPOULOS, I. Stabilized space-time finite element methods of parabolic evolution problems. Tech. Rep. 2017-19, Johann Radon Institute for Computational and Applied Mathematics (RICAM), Linz, 2017.
- [27] URBAN, K., AND PATERA, A. T. An improved error bound for reduced basis approximation of linear parabolic problems. *Math. Comp.* 83, 288 (2014), 1599–1615.

Technical Reports of the Doctoral Program

“Computational Mathematics”

2017

- 2017-01** E. Buckwar, A. Thalhammer: *Importance Sampling Techniques for Stochastic Partial Differential Equations* January 2017. Eds.: U. Langer, R. Ramlau
- 2017-02** C. Hofer, I. Touloupoulos: *Discontinuous Galerkin Isogeometric Analysis for parametrizations with overlapping regions* June 2017. Eds.: U. Langer, V. Pillwein
- 2017-03** C. Hofer, S. Takacs: *Inexact Dual-Primal Isogeometric Tearing and Interconnecting Methods* June 2017. Eds.: B. Jüttler, V. Pillwein
- 2017-04** M. Neumüller, A. Thalhammer: *Combining Space-Time Multigrid Techniques with Multilevel Monte Carlo Methods for SDEs* June 2017. Eds.: U. Langer, E. Buckwar
- 2017-05** C. Hofer, U. Langer, M. Neumüller: *Time-Multipatch Discontinuous Galerkin Space-Time Isogeometric Analysis of Parabolic Evolution Problems* August 2017. Eds.: V. Pillwein, B. Jüttler
- 2017-06** M. Neumüller, A. Thalhammer: *A Fully Parallelizable Space-Time Multilevel Monte Carlo Method for Stochastic Differential Equations with Additive Noise* September 2017. Eds.: U. Langer, E. Buckwar
- 2017-07** A. Schafelner: *Space-time Finite Element Methods for Parabolic Initial-Boundary Problems with Variable Coefficients* September 2017. Eds.: U. Langer, B. Jüttler

2016

- 2016-01** P. Gangl, U. Langer: *A Local Mesh Modification Strategy for Interface Problems with Application to Shape and Topology Optimization* November 2016. Eds.: B. Jüttler, R. Ramlau
- 2016-02** C. Hofer: *Parallelization of Continuous and Discontinuous Galerkin Dual-Primal Isogeometric Tearing and Interconnecting Methods* November 2016. Eds.: U. Langer, W. Zulehner
- 2016-03** C. Hofer: *Analysis of Discontinuous Galerkin Dual-Primal Isogeometric Tearing and Interconnecting Methods* November 2016. Eds.: U. Langer, B. Jüttler
- 2016-04** A. Seiler, B. Jüttler: *Adaptive Numerical Quadrature for the Isogeometric Discontinuous Galerkin Method* November 2016. Eds.: U. Langer, J. Schicho
- 2016-05** S. Hubmer, A. Neubauer, R. Ramlau, H. U. Voss: *On the Parameter Estimation Problem of Magnetic Resonance Advection Imaging* December 2016. Eds.: B. Jüttler, U. Langer
- 2016-06** S. Hubmer, R. Ramlau: *Convergence Analysis of a Two-Point Gradient Method for Nonlinear Ill-Posed Problems* December 2016. Eds.: B. Jüttler, U. Langer

2015

- 2015-01** G. Grasegger, A. Lastra, J. Rafael Sendra, F. Winkler: *A Solution Method for Autonomous First-Order Algebraic Partial Differential Equations in Several Variables* January 2015. Eds.: U. Langer, J. Schicho
- 2015-02** P. Gangl, U. Langer, A. Laurain, H. Meftahi, K. Sturm: *Shape Optimization of an Electric Motor Subject to Nonlinear Magnetostatics* January 2015. Eds.: B. Jüttler, R. Ramlau
- 2015-03** C. Fürst, G. Landsmann: *Computation of Dimension in Filtered Free Modules by Gröbner Reduction* May 2015. Eds.: P. Paule, F. Winkler
- 2015-04** A. Mantzafllaris, H. Rahkooy, Z. Zafeirakopoulos: *Efficient Computation of Multiplicity and Directional Multiplicity of an Isolated Point* July 2015. Eds.: B. Buchberger, J. Schicho
- 2015-05** P. Gangl, S. Amstutz, U. Langer: *Topology Optimization of Electric Motor Using Topological Derivative for Nonlinear Magnetostatics* July 2015. Eds.: B. Jüttler, R. Ramlau
- 2015-06** A. Maletzky: *Exploring Reduction Ring Theory in Theorema* August 2015. Eds.: B. Buchberger, W. Schreiner

The complete list since 2009 can be found at
<https://www.dk-compmath.jku.at/publications/>

Doctoral Program

“Computational Mathematics”

Director:

Prof. Dr. Peter Paule
Research Institute for Symbolic Computation

Deputy Director:

Prof. Dr. Bert Jüttler
Institute of Applied Geometry

Address:

Johannes Kepler University Linz
Doctoral Program “Computational Mathematics”
Altenbergerstr. 69
A-4040 Linz
Austria
Tel.: ++43 732-2468-6840

E-Mail:

office@dk-compmath.jku.at

Homepage:

<http://www.dk-compmath.jku.at>